10323
NACA TN 3992

TECH LIBRARY KAFB, NM
0067064

NATIONAL ADVISORY COMMITTEE FOR AERONAUTICS

TECHNICAL NOTE 3992

CHARTS FOR ESTIMATING THE EFFECTS OF SHORT-PERIOD STABILITY CHARACTERISTICS ON AIRPLANE VERTICAL-ACCELERATION AND PITCH-ANGLE RESPONSE IN CONTINUOUS ATMOSPHERIC TURBULENCE

By Kermit G. Pratt and Floyd V. Bennett

Langley Aeronautical Laboratory
Langley Field, Va.

Washington
June 1957

AFL 2811

TECH LIBRARY KAFB, NM

0067064

NATIONAL ADVISORY COMMITTEE FOR AERONAUTICS

TECHNICAL NOTE 3992

CHARTS FOR ESTIMATING THE EFFECTS OF SHORT-PERIOD STABILITY CHARACTERISTICS ON AIRPLANE VERTICAL-ACCELERATION AND PITCH-ANGLE RESPONSE IN CONTINUOUS ATMOSPHERIC TURBULENCE

By Kermit G. Pratt and Floyd V. Bennett

SUMMARY

Charts are presented for estimating the effects of variations in short-period stability characteristics of a rigid airplane on its root-mean-square vertical-acceleration and pitch-angle response to continuous atmospheric turbulence. From these charts the root-mean-square quantities in dimensionless form can be estimated for values of four other dimensionless parameters which describe the airplane short-period stability characteristics and the scale of atmospheric turbulence. The trends of the root-mean-square responses with each of the four parameters are discussed in terms of two significant combinations of the parameters involved. The charts are best suited for application to rigid unswept-wing airplanes of not more than 200-foot wing span flying at low subsonic speeds. It is believed, however, that useful estimates of first-order effects can be made for airplanes with other wing plan forms flying at high speeds. Analysis of the charts indicates that the variations of the vertical acceleration and pitch angle with the other parameters are largely determined by the damping ratio of the airplane and a relative-turbulence scale. Some examples of the application of these charts show that the vertical-acceleration response of a moderate-speed unswept-wing fighter airplane is increased by a rearward shift in the center of gravity, is not changed significantly with a change in altitude if the equivalent airspeed and true turbulence intensities are constant (effects of changes in Mach number are not included), and is increased by an increase in the geometric scale.

A comparison of the root-mean-square vertical-acceleration response of an airplane free to be disturbed in vertical and pitching motion with that of an airplane free to be disturbed only in vertical motion (nonpitching) indicates that the responses are similar for a nearly critically damped airplane. The acceleration response of an airplane with a very low damping ratio may greatly exceed the response of a nonpitching airplane. However, the vertical acceleration of an airplane having satisfactory handling qualities may in many cases be less than that of a nonpitching airplane.

INTRODUCTION

Variations of longitudinal stability characteristics may cause appreciable changes in the response (motions, loads, stresses, etc.) of an airplane flying in atmospheric turbulence. Until recently, analyses of these effects (some of which are summarized in ref. 1) disregarded the continuous nature of the turbulence, partly because of the large efforts required for a more realistic treatment, and considered, instead, only discrete gusts. This approach was considered to be unsatisfactory in many cases, particularly for airplanes having unusual longitudinal stability characteristics, such as low damping in pitch.

In recent years, the difficulties which led to use of discrete gust analysis have been overcome to a large extent by developments in the theory of generalized harmonic analysis (refs. 2 to 8) which permit the consideration of the continuous nature of turbulence. Within the framework of generalized harmonic analysis the airplane response to turbulence is described in terms of statistical or average quantities. The most important of these quantities is the root-mean-square value, which provides a simple measure of the response intensity and in the case of a Gaussian process completely specifies the probability distribution. (See ref. 4.)

The root-mean-square vertical acceleration of a rigid airplane has previously been calculated by means of generalized harmonic analysis for a few combinations of the damping and natural-frequency parameters of short-period longitudinal stability (ref. 4). The manner in which these root-mean-square values may be affected by changes in the short-period stability characteristics has been verified experimentally (ref. 5) to a limited extent. In reference 6, the root-mean-square response calculations have been extended to include pitching velocity as well as vertical acceleration. The results of these calculations indicate the effect of successive changes in some parameters which contribute to the short-period stability characteristics.

In the study of airplane response to continuous turbulence reported in reference 7, the root-mean-square vertical and pitching motions in dimensionless form were expressed as functions of only four other nondimensional parameters, namely, an airplane mass parameter, a short-period damping parameter, a short-period damped-natural-frequency parameter, and a turbulence-scale parameter. The simplification afforded by the formulation of the problem in terms of these parameters makes practicable the preparation of charts for the estimation of the effects of general variations in longitudinal stability characteristics of an airplane on its response to turbulence. The purpose of this report is to present charts from which the root-mean-square vertical acceleration and pitch angle in dimensionless form can be determined for values of the remaining four

parameters. The ranges of values selected for the parameters are believed to include values corresponding to those for most rigid unswept-wing airplanes and missiles likely to be considered in the near future.

In addition to the presentation of the charts, the trends in the variations of the root-mean-square airplane responses with each of the four independent parameters are discussed in terms of extreme values of two physically significant combinations of the four parameters. Also, the effects of pitching motion on the vertical acceleration of the airplane are indicated by a comparison of the present results with those obtained for an airplane free to be disturbed in vertical motion only. The application of the charts is illustrated by means of several examples, which were chosen to indicate the effects on the vertical-acceleration response of changes in the airplane center of gravity, in altitude, and in the size of the airplane.

SYMBOLS

a_n nondimensional normal or vertical acceleration, $\ddot{z}/g$

$a_{n,s}$ reference nondimensional normal or vertical acceleration, $\dfrac{qSC_{L_\alpha w}}{WU}$

$a_{n,r}$ vertical-acceleration ratio, $a_n/a_{n,s}$

C_{L_α} airplane lift-curve slope per radian

$C_{L_{\alpha,w}}$ wing lift-curve slope per radian

$C_{L_{\alpha,t}}$ tail lift-curve slope per radian

C_m pitching-moment coefficient, $M/qS\bar{c}$

C_{m_α} longitudinal static stability derivative, $\partial C_m/\partial\alpha$

$C_{m_{\dot{\alpha}}}$ pitching-moment coefficient per nondimensional unit rate of change of angle of attack, $\dfrac{\partial C_m}{\partial\left(\dfrac{\bar{c}\dot{\alpha}}{2U}\right)}$

C_{m_q} pitch damping derivative, $\dfrac{\partial C_m}{\partial\left(\dfrac{\dot{\theta}\bar{c}}{2U}\right)}$

c	local wing chord
$\bar{c}$	mean aerodynamic wing chord, $\frac{2}{S}\int_0^{b/2} c^2 dy$, ft
$\bar{c}_t$	mean aerodynamic tail chord, ft
g	acceleration due to gravity, ft/sec^2
h	pressure altitude, ft
H_O^I	frequency-response function for output response O to input disturbance I
k	reduced-frequency parameter, $\omega\bar{c}/2U$, radians/semichord
k_d	damped-natural-frequency parameter, $\omega_d\bar{c}/2U$, radians/semichord
k_o	undamped-natural-frequency parameter, $\omega_o\bar{c}/2U$, radians/semichord
L	turbulence scale, ft
l_t	distance from airplane center of gravity to aerodynamic center of horizontal tail, ft
l_w	distance from airplane center of gravity to aerodynamic center of wing-fuselage combination, ft
M	pitching moment about center of gravity, ft-lb
m	airplane mass, slugs
q	dynamic pressure, lb/sq ft
r	radius of gyration in pitch, ft
S	wing area, sq ft
S_t	horizontal-tail area, sq ft
s	turbulence-scale parameter, $2L/\bar{c}$
$T_{1/2}$	time for disturbance to damp to one-half amplitude, sec
U	airspeed, ft/sec
W	airplane weight, lb

w	vertical component of turbulence velocity, ft/sec
y	distance along wing span
z	vertical displacement, positive upward
z'	displacement normal to airplane, positive downward
α	angle of attack
α_T	angle of attack due to vertical component of turbulence, w/U, radians
γ	short-period damping parameter, $\kappa\nu$
ϵ	downwash angle, radians
η	tail-efficiency factor
κ	mass parameter, $\frac{8m}{C_{L_\alpha}\rho S\bar{c}}$
θ	pitch angle, positive nose upward, radians
θ_s	reference pitch angle, radians
θ_r	pitch-angle ratio, θ/θ_s
$\ddot{\theta}_s$	reference pitching acceleration, radians/sec^2
$\ddot{\theta}_{s,o}$	reference pitching acceleration (due to gust only), radians/sec^2
$\ddot{\theta}_r$	pitching-acceleration ratio, $\ddot{\theta}/\ddot{\theta}_s$
ν	nondimensional reciprocal of the time for disturbance to damp to one-half amplitude, $\frac{\bar{c}\log_e 2}{2UT_{1/2}}$
ζ	damping ratio
ρ	air density, slugs/cu ft
σ	root-mean-square value
$\hat{\Phi}(k)$, $\Phi(\omega)$	power spectra

$\phi(k)$, $\phi(\omega)$ unsteady-lift functions for gust penetration

ω frequency, radians/sec

ω_d damped natural frequency, radians/sec

ω_o undamped natural frequency, radians/sec

Notation:

$\dot{}$ first derivative with respect to time, d/dt

$\ddot{}$ second derivative with respect to time, d^2/dt^2

$|\ |$ absolute value of complex quantity

$'$ pertains to body-fixed stability axes

Subscripts or superscripts:

2 twice basic scale

40 at 40,000 feet

a at rearward center-of-gravity position

f at forward center-of-gravity position

I pertains to input

O pertains to output

sl at sea level

w pertains to vertical component of turbulence velocity

$a_{n,r}$ vertical-acceleration ratio

α_T pertains to angle of attack due to vertical component of turbulence

θ_r pitch-angle ratio

METHOD AND SCOPE OF CALCULATIONS

Method of Analysis

The charts of the root-mean-square dimensionless vertical acceleration and pitch angle to be presented herein were calculated from essentially the expressions for the corresponding quantities given in reference 7. These expressions, which were derived on the basis of the theory of generalized harmonic analysis, are rederived in this section, and some additional parameters, which find application in the following sections, are introduced.

According to the theory of generalized harmonic analysis the mean-square value of the output of a linear system subjected to a stationary random input, that is, an input process with statistical characteristics which are invariant with time, can be expressed as follows (ref. 4):

$$\sigma_0{}^2 = \int_0^\infty \left|H_0^I(\omega)\right|^2 \Phi_I(\omega)d\omega \tag{1}$$

This expression states that the mean-square value of the output is equal to the integral of the product of the input-power spectrum $\Phi_I(\omega)$ and the absolute square of the frequency-response function of the system $\left|H_0^I(\omega)\right|^2$. The power spectrum is a continuous spectrum of the contribution of each frequency to the total value of the mean-square of the random-input function. The frequency-response function describes the response of the system to a sinusoidal input of unit amplitude. In the cases of interest in this report the output 0 represents airplane vertical or pitching acceleration or pitch angle, and the input I represents the vertical component of the turbulent velocity.

Frequency-Response Functions

Equations of motion.- The frequency-response functions utilized herein were obtained from reference 7: They represent solutions of the equations of longitudinal motion (the effects of changes in airspeed being ignored) for an airplane flying in an atmosphere in which the vertical component of velocity varies sinusoidally in the direction of flight and is constant along the span of the wing at any instant.

These equations of motion are based on the assumptions commonly made in a longitudinal short-period stability analysis of rigid airplanes (ref. 9, for instance), in which an airplane is considered free to pitch and plunge (move in a direction normal to a longitudinal reference axis

of the airplane). Also, the effect of unsteady flow due to gust penetration on the airplane moments was assumed to be the same as the effect on the lift. (The lag in the application of the gust between wing and tail was, therefore, neglected.) Turbulence velocities were assumed to be small compared to the airspeed (so that the angle w/U in radians is numerically equal to its tangent), and only the vertical component of turbulence velocity was assumed to be important.

The equations of motion in operational form are then

$$\begin{bmatrix} i\omega + \dfrac{qSC_{L_\alpha}}{mU} & -i\omega U \\ \dfrac{-i\omega qS\bar{c}^2}{2mr^2U^2} C_{m_{\dot{\alpha}}} - \dfrac{qS\bar{c}}{mr^2U} C_{m_\alpha} & -\omega^2 - \dfrac{i\omega qS\bar{c}^2}{2mr^2U} C_{m_q} \end{bmatrix} \begin{Bmatrix} \dot{z}' \\ \theta \end{Bmatrix} = \phi(\omega) \begin{Bmatrix} \dfrac{-qSC_{L_\alpha}}{mU} \\ \dfrac{qS\bar{c}}{mr^2U} C_{m_\alpha} \end{Bmatrix} w \tag{2}$$

The preceding equations are based on stability axes, that is, body-fixed coordinates initially normal and parallel to the relative air velocity for undisturbed flight. These axes rotate about the origin as the airplane pitches and the acceleration $\ddot{z}'$ is not, therefore, the actual airplane acceleration. In most practical problems, such as load determination, the actual acceleration in the direction of the Z'-axis is required. Under the short-period stability assumptions, this quantity is substantially the same as the absolute acceleration $\ddot{Z}$ along a vertical axis of a coordinate-system translating at the speed of flight but otherwise fixed in space. The expression for vertical acceleration is

$$\ddot{Z} = -\ddot{z}' + U\dot{\theta} \tag{3}$$

The two sets of axes are shown in figure 1. As is well known, the dynamic response of the system described by equations (2) is oscillatory in nature and can be described as a function of natural frequency and damping parameters.

Dimensionless frequency-response functions.- In reference 7, solutions of the equations were obtained for the absolute square of the frequency-response functions, $\left|H^w_{\ddot{Z}}(\omega)\right|^2$ and $\left|H^w_{\ddot{\theta}}(\omega)\right|^2$.

By use of the relations

$$\alpha_T = w/U$$

$$k = \frac{\omega\bar{c}}{2U}$$

$$\theta = -\frac{\ddot{\theta}}{\omega^2}$$

together with

$$a_n = \ddot{z}/g \tag{4}$$

$$a_{n,s} = \frac{qSC_{L_\alpha}w}{mgU} \tag{5}$$

$$a_{n,r} = a_n/a_{n,s} \tag{6}$$

$$\theta_r = \theta/\theta_s \tag{7}$$

$$\theta_s = -\alpha_T \frac{\left[\frac{1}{\kappa^2}(\gamma - 2)^2 + k_d^2\right]}{k_d^2 + \frac{\gamma^2}{\kappa^2}} \tag{8}$$

$$\ddot{\theta}_r = \ddot{\theta}/\ddot{\theta}_s \tag{9}$$

$$\ddot{\theta}_s = \ddot{\theta}_{s,o}\left[1 - \frac{\rho S\bar{c}C_{L_\alpha}C_{m_{\dot{\alpha}}}}{4mC_{m_\alpha}}\right] \tag{10}$$

and

$$\ddot{\theta}_{s,o} = \frac{qS\bar{c}C_{m_\alpha}w}{mr^2U} \tag{11}$$

the functions $\left|H_{\ddot{z}}^{w}(\omega)\right|^2$ and $\left|H_{\ddot{\theta}}^{w}(\omega)\right|^2$ can be converted to the dimensionless forms $\left|H_{a_{n,r}}^{\alpha_T}(k)\right|^2$, $\left|H_{\theta_r}^{\alpha_T}(k)\right|^2$, and $\left|H_{\ddot{\theta}_r}^{\alpha_T}(k)\right|^2$. The parameters $a_{n,s}$, θ_s, and $\ddot{\theta}_{s,o}$ are reference values; $a_{n,s}$ may be interpreted as the nondimensional vertical acceleration that would result solely from the lift force associated with the maximum value of the sinusoidal vertical velocities; θ_s is the zero frequency value of θ; and $\ddot{\theta}_{s,o}$ may be interpreted as the pitching acceleration that would result solely from the moments associated with the maximum value of the sinusoidal vertical velocities. The quantities in the brackets in equations (8) and (10) may be regarded as coupling factors for the effect of vertical motion. The parameters κ, γ, and $k_{\dot{\alpha}}$ which appear in the brackets are nondimensional and are defined as follows:

The parameter κ is a mass parameter defined in reference 10, which will be recognized as four times the mass parameter used in discrete gust analyses as a vertical-motion damping coefficient (ref. 1), namely,

$$\kappa \equiv \frac{8m}{\rho S\bar{c}C_{L_\alpha}} \tag{12}$$

The parameter γ is defined as

$$\gamma \equiv \kappa\nu \tag{13}$$

where $1/\nu$ is a dimensionless form of the time for disturbed motion to subside to one-half amplitude, namely,

$$\nu \equiv \frac{\bar{c}\ \log_e 2}{2UT_{1/2}} \tag{14}$$

where in turn

$$\frac{\log_e 2}{T_{1/2}} = \frac{qS}{2Um}\left[C_{L_\alpha} - \frac{\bar{c}^2}{2r^2}\left(C_{m_q} + C_{m_{\dot{\alpha}}}\right)\right] \tag{15}$$

The parameter γ therefore can also be expressed as

$$\gamma = \left[1 - \frac{\bar{c}^2}{2r^2} \frac{\left(C_{m_q} + C_{m_{\dot{\alpha}}}\right)}{C_{L_\alpha}}\right] \tag{16}$$

The parameter k_d is a dimensionless form of the damped natural frequency of short-period motion, that is,

$$k_d = \frac{\omega_d \bar{c}}{2U}$$

The dimensionless damped natural frequency can be expressed in terms of the dimensionless undamped natural frequency k_o as

$$k_d = \sqrt{k_o{}^2 - \frac{\gamma^2}{\kappa^2}} \tag{17}$$

where

$$k_o = \sqrt{-\frac{\bar{c}^2}{r^2} \frac{1}{\kappa C_{L_\alpha}}\left(\frac{2}{\kappa} C_{m_q} + C_{m_\alpha}\right)} \tag{18}$$

An additional parameter involving k_d and γ/κ which will be utilized subsequently is the damping ratio ζ, the ratio of damping to critical damping, defined by

$$\zeta \equiv \frac{\gamma/\kappa}{\sqrt{k_d{}^2 + \frac{\gamma^2}{\kappa^2}}} = \frac{\nu}{k_o} \tag{19}$$

The use of the parameters γ, ν, and κ requires some comment. Any two of them define the third. The combination ν and κ is probably the most significant from consideration of physical interpretation. The pair γ and κ was selected, however, in order to provide

a parameter, namely, γ, which is independent of airplane mass and to retain the identity of κ because it is a familiar fundamental parameter in the analysis of the response of an airplane free to be disturbed in the vertical direction only.

The expression for $\left|H_{a_{n,r}}^{\alpha_T}(k)\right|^2$ was obtained from equation (48a) in reference 7 by using the dimensionless parameters defined in the preceding relations and is given by

$$\left|H_{a_{n,r}}^{\alpha_T}(k)\right|^2 = \frac{\left|\phi(k)\right|^2\left[k^4 + 4\frac{\gamma^2}{\kappa^2}\left(1 - \frac{1}{\gamma}\right)^2 k^2\right]}{\alpha_T^2\left[k^4 - 2\left(k_d^2 - \frac{\gamma^2}{\kappa^2}\right)k^2 + \left(k_d^2 + \frac{\gamma^2}{\kappa^2}\right)^2\right]} \tag{20}$$

The function $\left|H_{\theta_r}^{\alpha_T}(k)\right|^2$ was obtained from equation (48b) in reference 7 as

$$\left|H_{\theta_r}^{\alpha_T}(k)\right|^2 = \frac{\left|\phi(k)\right|^2\left(k_d^2 + \frac{\gamma^2}{\kappa^2}\right)^2}{\alpha_T^2\left[k^4 - 2\left(k_d^2 - \frac{\gamma^2}{\kappa^2}\right)k^2 + \left(k_d^2 + \frac{\gamma^2}{\kappa^2}\right)^2\right]} \tag{21}$$

and an expression for $\left|H_{\dot{\theta}_r}^{\alpha_T}(k)\right|^2$ can be obtained in a similar manner.

Unsteady-lift function.- The effect of unsteady flow on the lift and moment due to gust penetration was represented in reference 7 and herein by the function $\phi(\omega)$, which appears in equation (2), and $\phi(k)$, which appears in equations (20) and (21). In reference 7 the following expression was used for this function:

$$\left|\phi(k)\right|^2 \approx \frac{1}{1 + 2\pi k} \tag{22}$$

The expression in equation (22) is an approximation of the unsteady lift on a wing in two-dimensional incompressible flow. As implied by the assumptions of stability analysis previously mentioned, the effects of the unsteady flow associated with the disturbed motions of the airplane were neglected.

Assumed Power Spectrum of Atmospheric Turbulence

The power spectrum used herein for α_T (where $\alpha_T = w/U$) on an airplane flying at speed U is that used in reference 8, namely,

$$\Phi_{\alpha_T}(\omega) = \sigma_{\alpha_T}{}^2 \frac{L}{\pi U} \frac{\left[1 + 3\left(L^2\omega^2/U^2\right)\right]}{\left[1 + \left(L^2\omega^2/U^2\right)\right]^2} \tag{23}$$

where σ_{α_T} is the root-mean-square value of the angle of attack due to the vertical component of turbulence velocity. Equation (23) can be rewritten in dimensionless form by using the relations

$$\hat{\Phi}_{\alpha_T}(k) = \Phi_{\alpha_T}(\omega)\frac{d\omega}{dk}$$

$$= \frac{2U}{\bar{c}}\Phi_{\alpha_T}(\omega)$$

and

$$s \equiv \frac{2L}{\bar{c}} \tag{24}$$

The resulting expression for the power spectrum is

$$\hat{\Phi}_{\alpha_T}(k) = \sigma_{\alpha_T}{}^2 \frac{s}{\pi} \frac{\left(1 + 3s^2k^2\right)}{\left(1 + s^2k^2\right)^2} \tag{25}$$

Final Equations

In terms of the dimensionless frequency-response functions given by equations (20) and (21), the unsteady-lift function in equation (22), and the power spectrum given by equation (25), the expressions for the mean-square values of $a_{n,r}$ and θ_r are

$$\sigma_{a_{n,r}}{}^2 = \int_0^\infty \left|H_{a_{n,r}}^{\alpha_T}(k)\right|^2 \hat{\Phi}_{\alpha_T}(k)dk \tag{26}$$

and

$$\sigma_{\theta_r}{}^2 = \int_0^\infty \left|H_{\theta_r}^{\alpha_T}(k)\right|^2 \hat{\Phi}_{\alpha_T}(k)dk \tag{27}$$

Presentation of Charts

Range of parameters.- Equations (26) and (27) were integrated in closed form and the rather lengthy expressions for $\sigma_{a_{n,r}}$ and σ_{θ_r} were evaluted by an automatic digital computer for the following ranges of values of k_d, κ, γ, and s:

$$0 \leqq k_d \leqq 0.2$$

$$40 \leqq \kappa \leqq 20,000$$

$$1 \leqq \gamma \leqq 10$$

$$50 \leqq s \leqq 2,000$$

The upper limits of these parameters were chosen to be appreciably higher than the largest values found in a survey of contemporary airplanes. The upper limit of κ, in particular, may seem excessively large, but this value may be approached by small heavily loaded missiles at high altitude. The lower limits of the parameters were set by various considerations. The limit of zero for k_d corresponds to critical damping. The limit of unity for γ is inherent in the definition of γ for stable airplanes. (See eq. (16).) It might be noted that tailless airplanes are often characterized by values of γ near unity. The lower limit of κ was chosen to include lightly loaded airplanes, such as sailplanes.

The limits of s require special mention. The value of s depends on the values of the turbulence scale L. Measurements of atmospheric turbulence from flight tests indicate that L is in the order of 1,000 feet, and on this basis the range of s would be from about 100 to 2,000 for large airplanes and small missiles, respectively. However, the lower limit of s was extended down to 50 to apply to values of L lower than 1,000 feet if further tests indicate their existence.

Index to charts.- The calculated values of $\sigma_{a_{n,r}}$ and σ_{θ_r} are presented as functions of k_d in figures 2 and 3, respectively, for various

values of γ, κ, and s. Log-log paper was used for the charts in order to make the presentation compact and to permit reading to a constant number of significant figures. It should be noted that values of $\sigma_{a_{n,r}}$ for $k_d = 0$ are presented as arrowheads to the left of the vertical axis of each $\sigma_{a_{n,r}}$ chart. One of these values on each chart, namely, that for $\gamma = 2$, is of special significance in that, as indicated in equation (8), the pitching motion is zero. These values, therefore, are for an airplane free to be disturbed only in vertical motion and are comparable to those presented in reference 10. The values of $\sigma_{a_{n,r}}$ for $k_d = 0$ and $\gamma = 2$ are functions of κ and s only and are presented as a function of κ in figure 4 as an extension of the information presented in reference 10. (Note that in ref. 10, s is defined as the inverse of s in this report.)

No special significance should be attached to the fact that the root-mean-square quantities in figures 2 and 3 are plotted as a function of k_d. This procedure was followed to minimize overlapping of the curves in order to provide ease in reading. Sample plots of the root-mean-square quantities are also given in figures 5 and 6 as a function of κ/γ, which is comparable to the presentation in figure 4.

Values of root-mean-square pitching-acceleration ratio $\sigma_{\ddot{\theta}_r}$ (for definition of $\ddot{\theta}_r$ see eq. (9)) were also calculated by use of an expression for the absolute square of the frequency-response function obtained from equation (48b) of reference 7 and are presented in table I. No charts have been prepared for these results.

Some Variations of Airplane Responses With Variations in the Dimensionless Parameters

The charts indicate that the variations of $\sigma_{a_{n,r}}$ and σ_{θ_r} with each of the parameters k_d, κ, γ, and s differ considerably for the innumerable combinations of the parameters which may result from various airplane configurations. These variations, however, can be systematized to a large extent by considering the variations of the σ's for extreme values of only two combinations of the four parameters. The two combinations are:

(1) The ratio of k_d to γ/κ

(2) The product of k_o and s

The first combination appears in the denominator that is common to equations (20) and (21). The relationship of k_d to γ/κ determines the ratio of damping to critical damping ζ and the undamped natural frequency parameter k_o. (See eqs. (17) and (19).) For $\frac{k_d}{\gamma/\kappa} \ll 1.0$ the value of $\zeta \approx 1.0$ and $k_o \approx \gamma/\kappa$. For $\frac{k_d}{\gamma/\kappa} \gg 1.0$ the value of $\zeta < 0.1$ and $k_o \approx k_d$.

The second significant combination of parameters with regard to the variations of the σ's, the product of k_o and s, determines the expansion or compression of the power-spectrum frequency scale relative to that of the frequency-response function.

For $k_o s \gg 1.0$, the frequency scale of the input spectrum is compressed relative to that of the frequency-response function so that the amplitude of the input spectrum varies inversely with the square of the reduced frequency beginning at a frequency that is a small fraction of the undamped natural frequency of the airplane. The condition $k_o s \gg 1.0$ is termed herein large relative-turbulence scale. The general relation between the vertical-acceleration and pitch-angle frequency-response moduli and the power spectrum for large relative-turbulence scale is indicated in figure 7(a).

For $k_o s \ll 1.0$ the frequency scale of the input spectrum is expanded relative to that of the frequency-response function so that the value of the input spectrum is nearly constant up to a frequency many times the undamped natural frequency of the airplane. This condition is termed herein small relative-turbulence scale. The general relation between the airplane frequency-response moduli and the power spectrum for small relative-turbulence scale is indicated in figure 7(b).

The condition of large relative-turbulence scale appears to apply for most airplanes and atmospheric conditions. Conditions approaching small relative-turbulence scale may be encountered occasionally. However, the portion of the turbulence spectrum associated with small relative-turbulence scale (the relatively constant portion at very long wavelengths) is subject to a large degree of uncertainty compared with the remainder of the spectrum. The root-mean-square quantities for small relative-turbulence scale are given primarily as an aid to the estimation of response trends for moderate values of relative-turbulence scale.

An appendix is included in which the extreme conditions of damping and relative-turbulence scale are shown to permit a simplification of the integrals in equations (26) and (27) so that short formulas (eqs. (A1) to (A6)) expressing the variations of $\sigma_{a_{n,r}}$ and σ_{θ_r} with

each of the parameters k_d, κ, γ, and s can be readily obtained for all extreme conditions except the nearly critically damped conditions for $\sigma_{a_{n,r}}$. In the case for critical damping the variations of $\sigma_{a_{n,r}}$ can be visualized qualitatively. The results for the extreme conditions are summarized in table II. The qualitative description of the variations of the σ's on the basis of the results in table II permits some generalization of results in studies of turbulence problems, as will be indicated in connection with some examples of chart application.

USE OF THE CHARTS

Chart Limitations

In the derivation of the equations from which the charts were calculated, some physical effects which are known to contribute to the response of an airplane to turbulence were purposely excluded and others were idealized in order to simplify the equations. Without these simplifications, the coverage of a wide range of airplane characteristics would require an impracticably large effort. The exclusion and idealization of these effects, however, imposes certain limitations on the use of the charts.

The effects pertinent to the response of an airplane to turbulence which have been excluded by the assumptions of short-period stability analysis are the large perturbations in airplane motion which may occur for airplanes having very low damping ratios and the unsteady lift accompanying a change in the angle of attack due to airplane disturbed motions (Wagner effect). Errors in the values of the $\sigma_{a_{n,r}}$ and σ_{θ_r} obtained from the charts due to large perturbations are thus a function of both ζ and σ_{α_T} and increase as σ_{α_T} is increased or ζ is reduced. The errors due to neglect of the Wagner effect are expected to increase with an increase in k_o.

The effect of neglecting the lag in application of the vertical turbulence velocities between the wing and tail is to decrease the root-mean-square response in much the same manner as would be obtained from an increase in damping ratio. This effect increases with an increase in tail effectiveness $\frac{\bar{c}^2}{r^2} \frac{1}{\kappa C_{L_\alpha}} \eta \frac{S_t}{S} C_{L_{\alpha,t}} \frac{l_t^2}{\bar{c}^2} \frac{d\epsilon}{d\alpha}$ and with both a decrease in k_o and an increase in κ for a given tail effectiveness.

The charts are based on an airplane flying with elevator neutral (fixed). The effect of a pilot is not included.

The input power spectrum used in the chart calculations is based on the assumption that the lift on the airplane is not appreciably affected by lateral (spanwise) variations of turbulence vertical velocities. It was pointed out in reference 7 that this assumption should provide satisfactory results for rigid airplanes having wing spans less than 100 feet. More recent information indicates that for the present purpose the spectrum should give satisfactory results even for airplanes with spans up to about 200 feet.

As was stated earlier this input power spectrum is subject to a large degree of uncertainty in the lower frequency region where it is relatively constant and, therefore, the results for the small values of relative-turbulence scale ($k_o s \ll 1$) are to be used only as an aid to the estimation of response trends for moderate and large values of relative-turbulence scale. The validity of the charts for values of $k_o s < 5$ is uncertain. A boundary for this condition is indicated on each chart in figures 2 and 3 except for charts for κ equal to 40 and 100 in figure 3. The curves for κ of 40 and 100 are too crowded to permit the insertion of a clearly defined boundary.

The basic assumptions and the choice of unsteady-lift functions used in the calculation of the charts thus imply that the charts are most applicable to rigid unswept-wing airplanes of not much more than 200-foot wing span flying at low subsonic speeds. It is believed, however, that useful estimates of changes in stability characteristics can be made for fairly rigid airplanes with wings of other plan form, such as swept or triangular flying at high subsonic and supersonic speeds. In general the charts presented herein (figs. 2 and 3) are best suited for the estimation of effects of changes in short-period stability characteristics on the root-mean-square vertical acceleration and pitch angle rather than for determining the magnitude of the root-mean-square quantities for a given set of airplane and turbulence parameters. The use of the charts to estimate the effects of such changes tends to minimize errors arising from simplifying assumptions and uncertainties in values of stability parameters.

Evaluation of Required Parameters

Stability parameters.- The stability parameters k_d and γ may be obtained from ω_d and $T_{1/2}$, which in turn may be determined from flight tests of an existing full-scale or model airplane, or else k_d and γ may be calculated from equations (16) to (18) in which values of the stability derivatives C_{L_α}, C_{m_α}, $C_{m_{\dot{\alpha}}}$, and C_{m_q} are obtained from whatever source is considered most reliable. The mass parameter κ is usually calculated by using values of C_{L_α} either measured or calculated.

Inasmuch as all airplane structures are flexible to a degree, calculations of the stability derivatives should include static aeroelastic effects. (Quasi-static aeroelastic effects, that is, those which arise from the structural deformation caused by the inertia loads in a uniform normal acceleration, can be included in the same way. See ref. 11, for instance.) The completely dynamic response of airplane structures, which includes inertia loads based on the local accelerations, cannot be taken into account in the use of the present charts and the results obtained therefrom will be subject to increasing errors as the natural frequencies and damping ratios decrease in values and as the static deflections of the natural structural modes increase in value.

Scale of turbulence.- The evaluation of the turbulence-scale parameter s requires that a value of L be selected. As mentioned elsewhere, little is known as to what variations in the value of L may occur or what meteorological conditions may affect the value of L. Some available information suggests that L is in the vicinity of 1,000 feet.

Examples of Chart Application

Three examples are presented to illustrate application of the charts and to provide information on some typical turbulence-response problems. They illustrate, respectively, the effect on vertical acceleration of changing the airplane center-of-gravity position, the altitude, and the geometric scale. The same basic airplane configuration was used in all three examples. The configuration chosen is that of a moderate-speed unswept-wing fighter airplane for which some flight test results were reported in reference 5. The pertinent characteristics of the basic airplane are listed in table III.

Change in airplane center of gravity.- The change in center of gravity was taken to be a rearward shift amounting to 6.6 percent of the mean aerodynamic chord of the wing. This change, together with slight changes in weight and radius of gyration indicated in table IV, was chosen to be the same as the value used in flight tests of the fighter airplane considered in reference 5. Values of κ, γ, and k_d listed in table IV for both center-of-gravity positions indicate that only k_d is appreciably affected by the center-of-gravity change. Values of $\sigma_{a_{n,r}}$ obtained from the charts by graphical interpolation for $s = 297$, which corresponds to $L = 1{,}000$ feet, and for the tabulated values of κ, γ, and k_d are also presented in table IV. The ratio of $\sigma_{a_{n,r}}$ for center of gravity rearward to that for center of gravity forward was found to be 1.045, from which the root-mean-square vertical acceleration was found to increase about 7.5 percent as the center of gravity was changed from the front to the rear position.

The results of the flight tests and calculations reported in reference 5 indicate increases in σ_{a_n} of about 10 and 13 percent, respectively. The differences between the results from the charts and from the calculations of reference 5 show, to a certain extent, the effects of unsteady lift due to a change in angle of attack (Wagner function) and of lag in application of the turbulence velocities between the wing and tail. These effects were accounted for in the calculations of reference 5, but, as previously indicated, were not included in the calculation of the charts. A comparison of the calculated results on this basis is not, however, completely clear-cut because the input power spectrum used in reference 5 was somewhat different from the spectrum used herein.

The present results together with those from reference 5 indicate that rearward shift in center of gravity results in a moderate increase in $\sigma_{a_{n,r}}$ for the airplane considered.

Some generalization concerning the effect of a change in center-of-gravity position can be made on the basis of the information given in tables II and III. A pure shift of center-of-gravity position produces little change in γ (at least for airplanes with tails) and no change in κ or s. A shift in the center-of-gravity position, however, may produce a change in k_d; a rearward shift tends to reduce k_o. For a nearly critically damped airplane $\sigma_{a_{n,r}}$ is nearly independent of k_d and, consequently, a change in center-of-gravity position should cause no appreciable change in the airplane response. For lightly damped airplanes ($\zeta < 0.1$) the reduction in k_d which accompanies a rearward center-of-gravity shift should cause a proportional decrease in vertical-acceleration response for small relative-turbulence scales ($k_o s \ll 1.0$). For large relative-turbulence scales, the reduction in k_d should cause a moderate increase in vertical-acceleration response. The conditions and the results of the numerical example given favor the last category cited.

Change in altitude.- The change in altitude selected was from sea level to 40,000 feet. The equivalent airspeed and the true turbulence intensity were assumed to be invariant with altitude. Effects of Mach number changes were not considered. As indicated in table V, wherein are listed the quantities which change with altitude, the mass parameter κ is increased about four times at 40,000 feet, whereas the damped natural-frequency parameter k_d is reduced to about one-half of the sea-level value. The ratio of acceleration at 40,000 feet to sea-level acceleration indicates that there is no appreciable change in vertical acceleration with altitude for the example airplane, provided that the turbulence intensity is independent of altitude.

As a matter of interest, the effect of pitching motion on the variations in acceleration response with altitude was indicated by comparing the preceding acceleration data with that for a nonpitching airplane. The latter data were obtained from the charts for $k_d = 0$ (for an airplane with γ nearly 2). It was found that the root-mean-square vertical acceleration for the nonpitching airplane was about 20 percent lower at 40,000 feet than at sea level.

Some generalization of the effects of altitude change on the response of the pitching airplane can be made. It can be shown by using equation (A1) in the appendix that the root-mean-square vertical acceleration for the lightly damped airplane and for small relative-turbulence scale ($k_o s \ll 1.0$) varies directly in proportion to the square root of air density. For large relative-turbulence scale, it can be shown by using equation (A2) that the vertical acceleration for the lightly damped airplane is nearly independent of changes in air density except for unsteady-lift effects which cause a small increase in acceleration with a decrease in air density that becomes more pronounced with an increase in the value of k_d at sea level. It appears impractical to extend generalization to the behavior of the acceleration response for airplanes which are nearly critically damped. For this damping condition, the trend of $\sigma_{a_{n,r}}$ with changes in air density is in opposition to the trend of $a_{n,s}$ with changes in air density and, therefore, specific cases must be determined. In many practical cases, effects of Mach number changes should not be neglected as they were in this example.

Change in airplane size.- A comparison was made of the vertical-acceleration responses of the basic airplane and an airplane twice its size. The airplanes were assumed to be dynamically similar, that is, values of $a_{n,s}$, κ, γ, and k_d were unchanged. As indicated in table VI the turbulence-scale parameter s is changed, however, as a result of the change in the wing reference chord. The 2:1 increase in airplane scale resulted in a 35 percent increase in $\sigma_{a_{n,r}}$ and in σ_{a_n}. In general, as shown in table II an increase in airplane size will be accompanied by a decrease in σ_{a_n} for a small relative-turbulence scale and by an increase in σ_{a_n} for a large relative-turbulence scale. The results of the numerical example are in agreement with the latter relation.

COMPARISON WITH NONPITCHING AIRPLANE

In the past, gust loads on airplanes, with the exception of those of unusual configurations, have generally been calculated on the assumption

(based on results of discrete gust analysis and on gust-tunnel tests summarized in ref. 1) that the effect of pitching motion on vertical accelerations is, if not necessarily negligible, at least nearly the same for all airplanes. In other words, the accelerations have been calculated on the basis of vertical-motion response only and, consequently, the accelerations are determined solely by the mass parameter κ, except that for continuous-turbulence calculations the scale parameter s enters as well. (See ref. 10.) This procedure has been considered to be applicable only to airplanes having satisfactory handling qualities. It is, therefore, of interest to compare the general results of the study of the effects of short-period stability characteristics with those for the condition of no pitch and also to examine these results in the light of a satisfactory handling-qualities criterion.

Effects of nearly critical and nearly zero damping ratios.- It has been pointed out previously that the particular condition of $k_d = 0$ and $\gamma = 2$ represents the no-pitch case treated in reference 10 and that values of $\sigma_{a_{n,r}}$ for the condition of $0 < \frac{k_d}{\gamma/\kappa} \ll 1.0$ (nearly critically damped) and $\gamma = 2$ are nearly identical to those for the no-pitch case. Observations of the charts (fig. 2) indicate that, for values of γ greater than 2 and for a given value of κ, the values of $\sigma_{a_{n,r}}$ for the nearly critically damped airplane are always less than the values for the no-pitch case. For values of γ between 1 and 2, the values of $\sigma_{a_{n,r}}$ for a given value of κ are higher than those for the no-pitch case but never exceed the maximum value with respect to κ for the no-pitch case. For the airplane with a very low damping ratio $\frac{k_d}{\gamma/\kappa} \gg 1.0$ the values of $\sigma_{a_{n,r}}$ may in some cases greatly exceed values of $\sigma_{a_{n,r}}$ for the no-pitch condition. (See fig. 2(u).)

Handling-qualities boundary.- The handling qualities of an airplane are generally considered satisfactory if a disturbed motion of the airplane decays to a stipulated fraction of its initial magnitude in less than a certain number of cycles. A commonly used condition is one-tenth of the initial magnitude in less than one cycle. The handling-qualities criterion can be expressed as a function of the damping ratio only and for the particular case cited, the corresponding damping ratio, $\zeta \geqq 0.345$. This damping ratio is not nearly critical by the criterion of $\frac{k_d}{\gamma/\kappa} \ll 1.0$ $\left(\text{in this case } \frac{k_d}{\gamma/\kappa} \leqq 2.73\right)$; nevertheless, this restriction when applied to

the curves presented in figure 2 (the boundary is indicated on the charts) serves in general to limit $\sigma_{a_{n,r}}$ to values equal to or less than those for the no-pitch condition. Exceptions exist for $\gamma < 2$ under all conditions and for values of $\gamma > 2$ at small values of s; however, even for these conditions, the values of $\sigma_{a_{n,r}}$ remain below unity. For damping ratios appreciably lower than that set by the handling-qualities criterion, the values of $\sigma_{a_{n,r}}$ may reach indefinitely large values for small values of s.

The preceding results tend to corroborate a conclusion reached in discrete gust analyses; namely, that, for airplanes having satisfactory handling qualities, conservative values of the vertical accelerations due to gusts can generally be calculated on the basis of vertical-motion response only.

CONCLUDING REMARKS

Charts have been presented for estimating the effects of variations in short-period stability characteristics of a rigid airplane on its root-mean-square vertical-acceleration and pitch-angle response to continuous atmospheric turbulence. From these charts the root-mean-square quantities in dimensionless form can be determined for values of four other dimensionless parameters; namely, an airplane mass parameter κ, a short-period damping parameter γ, a short-period damped-natural-frequency parameter k_d, and a turbulence-scale parameter s. Analysis of the equations from which the charts were calculated indicates that the variations of the vertical acceleration and pitch angle with the other parameters are largely determined by two other quantities; namely, the damping ratio of the airplane which may be expressed in terms of κ, γ, and k_d, and the relative-turbulence scale which may be expressed in terms of the undamped-natural-frequency parameter k_o and the turbulence-scale parameter s. Formulas are presented for some extreme conditions of damping ratio and relative-turbulence scale to facilitate some qualitative generalization of trends of root-mean-square response with changes in k_d, κ, γ, and s.

The charts are best suited for the estimation of the effects of changes in short-period stability characteristics of rigid unswept-wing airplanes of not more than 200-foot wing span flying at low subsonic speeds. It is believed, however, that useful estimates of first-order effects can be made for airplanes with wings of other plan forms flying at high speeds.

Examples of chart application have been presented to show the effects on vertical acceleration of changes in airplane center of gravity, in altitude, and in geometric scale. The results indicate that, for the particular airplane considered, the vertical acceleration is increased by a rearward shift in the center of gravity; no significant change in vertical acceleration occurs for a change in altitude from sea level to 40,000 feet, if the equivalent airspeed and true turbulence velocities are constant and effects of Mach number are not considered; and that the acceleration is increased as the geometric scale of the airplane is increased.

A comparison of the root-mean-square vertical-acceleration response of an airplane free to be disturbed in vertical and pitching motions with that of an airplane free to be disturbed only in vertical motion (nonpitching) indicates that the responses are very nearly the same for a nearly critically damped airplane having a short-period damping parameter γ of 2. For values of γ greater than 2, the vertical acceleration response of the nearly critically damped airplane is always less than that for the airplane for which $\gamma = 2$. On the other hand, the vertical-acceleration response of an airplane with a very low damping ratio may greatly exceed the response of an airplane which is free to be disturbed in vertical motion only.

The application of a satisfactory-handling-qualities criterion to the vertical-acceleration charts indicates that in many cases the vertical-acceleration response of an airplane having satisfactory handling qualities is less than that for an airplane free to be disturbed only in vertical motion and in no case does it exceed the reference acceleration response which ignores the effects of airplane motion and of unsteady lift.

Langley Aeronautical Laboratory,
National Advisory Committee for Aeronautics,
Langley Field, Va., January 29, 1957.

APPENDIX

ANALYSIS OF AIRPLANE RESPONSES AS AFFECTED BY VARIATIONS IN THE DIMENSIONLESS PARAMETERS

The charts presented herein indicate that the manner in which $\sigma_{a_{n,r}}$ or σ_{θ_r} varies with each of the parameters k_d, κ, γ, and s differs considerably for the many possible combinations of the parameters which may result from various airplane configurations. This appendix shows that these variations can be systematized to a large extent by considering the variations of the σ's for extreme values of the airplane damping ratio and the relative-turbulence scale previously described in the text. These extreme conditions permit a simplification of the integrals in equations (26) and (27) so that short formulas expressing the variations of $\sigma_{a_{n,r}}$ and σ_{θ_r} with each of the parameters can be obtained readily for all extreme conditions except the nearly critically damped conditions for $\sigma_{a_{n,r}}$. For this exception, the variations of $\sigma_{a_{n,r}}$ can be visualized qualitatively. The formulas are used in this appendix as a basis for discussion of the variations of the σ's and may also be directly useful in some cases.

Effect of the Various Parameters on the Vertical Acceleration

Effect of k_d on $\sigma_{a_{n,r}}$.- For values of k_d that are small compared to the ratio γ/κ $\left(\text{say } \frac{k_d}{\gamma/\kappa} < 0.1\right)$, the modulus of the frequency-response function and consequently the root-mean-square acceleration ratio $\sigma_{a_{n,r}}$ are practically independent of variations in k_d as indicated by equation (20). This characteristic is unaffected by changes in the value of k_o relative to s.

For values of $\frac{k_d}{\gamma/\kappa} > 10$ the system has very low damping ($\zeta < 0.1$) and a resonant peak of high amplitude is present in the transfer-function modulus. (See fig. 7.) The amplitude of the resonant peak is so great that the area represented by the integral (eq. (26)) is very nearly proportional to the area under the peak alone. This characteristic, together with the small width of the resonant peak, permits a simple approximation

of $\sigma_{a_{n,r}}$ by the multiplication of the integral of the absolute square of the transfer function alone by the values of the unsteady-lift function and the power spectrum at the resonant frequency $k_o \approx k_d$. This approximation is based on the approach outlined in equations (9) and (17) to (21) in reference 8 and yields, for a small relative-turbulence scale ($k_d s < 0.6$),

$$\sigma_{a_{n,r}} \approx \left[\frac{\left|\phi(k_d)\right|^2 k_d^2 \kappa s}{4\gamma}\right]^{1/2} \tag{A1}$$

and for a large relative-turbulence scale ($k_d s > 10$)

$$\sigma_{a_{n,r}} \approx \left[\frac{3\left|\phi(k_d)\right|^2 \kappa}{4\gamma s}\right]^{1/2} \tag{A2}$$

As indicated by equations (A1) and (A2), the variation of $\sigma_{a_{n,r}}$ with k_d for the very low damping conditions depends upon the relative-turbulence scale. For a small relative-turbulence scale $\sigma_{a_{n,r}}$ is indicated by equation (A1) to vary directly with k_d except for the effect of unsteady lift, which for most practical values of k_d produces a minor decrease in $\sigma_{a_{n,r}}$ with an increase in k_d. This characteristic arises from the combination of a flat power spectrum and an increase in amplitude of the resonant peak of the transfer-function modulus that accompanies a decrease in damping ratio as k_d increases. (See fig. 7(b).) For a large relative-turbulence scale $\sigma_{a_{n,r}}$ is indicated by equation (A2) to be independent of k_d except for the effect of unsteady lift which results in a moderate decrease in $\sigma_{a_{n,r}}$ with increasing values of k_d. This characteristic arises from the combination of a variation of resonant peak amplitude, which is identical to that for a small relative-turbulence scale, and a power spectrum that varies inversely with the square of k_d over a wide range of values of k_d. The increase in area under the resonant peak which occurs with an increase in k_d is nullified by the accompanying reduction in the value of the power spectrum at the resonant frequency. (See fig. 7(a).) The trends of $\sigma_{a_{n,r}}$ with k are summarized in table II.

Effect of κ and γ on $\sigma_{a_{n,r}}$.- The parameters κ and γ are indicated by equation (20) to affect the transfer function in the form of the ratios γ/κ and $1/\gamma$. The results shown in figure 5 indicate, however, that the contribution of the term containing $1/\gamma$, while appreciable for large values of γ/κ, does not affect the general trend of $\sigma_{a_{n,r}}$ with γ/κ.

For $\frac{k_d}{\gamma/\kappa} \ll 1.0$ the nearly critical damping results in a transfer-function modulus with a shape which is similar to the shape of the transfer-function modulus for an airplane free to be disturbed in the vertical direction only (nonpitching airplane). This similarity is not surprising, inasmuch as the nonpitching condition is obtained from the present equations for $k_d = 0$ and $\gamma = 2$, as has been pointed out previously. Consequently, the variation of $\sigma_{a_{n,r}}$ with γ/κ for the condition $\frac{k_d}{\gamma/\kappa} \ll 1.0$ will be similar to that for the nonpitching airplane.

Although no simple procedure for the calculation of the variation of $\sigma_{a_{n,r}}$ with γ/κ for the nonpitching airplane has been discovered, this variation can be estimated from an examination of the transfer-function modulus squared, which is obtained from equation (20) by setting $\gamma = 2$ and $k_d = 0$. The transfer-function modulus squared $\left|H_{a_{n,r}}^{\alpha_T}(k)\right|^2$ approaches the value of the unsteady-lift function squared $|\phi(k)|^2$ as k increases, and increasing values of κ cause $\left|H_{a_{n,r}}^{\alpha_T}(k)\right|^2$ to reach a given percentage of the unsteady-lift function squared at progressively lower frequencies. It follows, therefore, that $\sigma_{a_{n,r}}$ will increase with an increase in κ due to the increase in area under the product of the power spectrum and $\left|H_{a_{n,r}}^{\alpha_T}(k)\right|^2$. This variation, however, does not continue indefinitely. As κ approaches infinite values, the transfer-function modulus approaches the unsteady-lift function for all frequencies. The maximum value of $\sigma_{a_{n,r}}$ is, therefore, proportional to the square root of the area under the product of the power spectrum and the unsteady-lift function only. The asymptotic value of $\sigma_{a_{n,r}}$ with respect to κ is then a function of only the turbulence-scale parameter s and is always less than unity.

Examination of equation (20) indicates that a similar variation of $\sigma_{a_{n,r}}$ with κ (or κ/γ for a given value of γ) occurs for other values of γ when $k_d = 0$ and that the asymptotic values of $\sigma_{a_{n,r}}$ with respect to κ are the same for all values of γ. For the condition $0 < \frac{k_d}{\gamma/\kappa} \ll 1.0$, the variation of $\sigma_{a_{n,r}}$ with γ/κ will be nearly the same as that for $k_d = 0$. The asymptotic values do not apply for $k_d \neq 0$, however, inasmuch as, for very small values of γ/κ (large values of κ), k_d cannot then be small compared to this ratio.

The variation of $\sigma_{a_{n,r}}$ with γ for a given value of κ (the form of presentation in figure 2) can also be estimated from equation (20). An increase in γ increases the frequency at which $\left|H_{a_{n,r}}^{\alpha_T}(k)\right|^2$ reaches a given percentage of the unsteady-lift function and also increases the rate with respect to frequency at which this condition is approached. The former characteristic tends to prevail and reduces the area under $\left|H_{a_{n,r}}^{\alpha_T}(k)\right|^2$ and consequently tends to reduce $\sigma_{a_{n,r}}$. On the other hand, for a given value of γ/κ (the more physically significant parameter) $\sigma_{a_{n,r}}$ can be shown by similar reasoning to increase with an increase in γ for the nearly critically damped airplane (form of presentation in figs. 5(b) and 5(c)).

For $\frac{k_d}{\gamma/\kappa} \gg 1.0$ the presence of a high resonant peak in the modulus of the frequency-response function due to a very low damping ratio causes $\sigma_{a_{n,r}}$ to vary inversely with the square root of γ/κ for both small and large relative-turbulence scale. (See eqs. (A1) and (A2).) In equation (20) it can be observed that for small values of γ/κ the numerator term containing both γ/κ and $1/\gamma$ becomes very small compared with the remaining terms, thus κ and γ affect the transfer function in the form of the ratio γ/κ only.

The characteristics indicated for variations of $\sigma_{a_{n,r}}$ with γ/κ and γ, together with those indicated earlier for variations with k_d, can be observed in figures 4 and 5. It should be noted that $\sigma_{a_{n,r}}$ is presented in these figures as a function of κ/γ rather than γ/κ. This presentation was used because $\sigma_{a_{n,r}}$ varies over a wider range with practical values of κ than it does with γ.

Figure 5(a) is presented to show the effects of a change in k_d as well as a change in κ. The value of γ is fixed at 2 in order that the nonpitching airplane may be represented by the curve $k_d = 0$.

Similar variations of $\sigma_{a_{n,r}}$ with κ/γ and k_d are found in figures 5(b) and 5(c) for $s = 50$ and 2,000, respectively. These figures, however, also indicate the effect of changes in γ for given values of κ/γ. At the lower values of κ/γ, which tend toward a critical damping ratio, the effect of a change in γ is maximum; an increase in γ for a given value of κ/γ increases $\sigma_{a_{n,r}}$. At the larger values of κ/γ the effect of changes in γ tends to become negligible. The trends of the variation of $\sigma_{a_{n,r}}$ with γ/κ and with γ for given values of γ/κ are summarized in table II.

Effect of s on $\sigma_{a_{n,r}}$.- The effect of an increase in the turbulence-scale parameter s depends upon the relative-turbulence scale. For a small relative-turbulence scale ($k_o s \ll 1.0$), $\sigma_{a_{n,r}}$ can be shown to increase directly with the square root of s regardless of the magnitude of the damping ratio. (For small damping ratio, see eq. (A1).) For large relative-turbulence scale, on the other hand, $\sigma_{a_{n,r}}$ decreases with an increase in s and varies inversely with the square root of s for the case of nearly zero damping ratio. (See eq. (A2).)

Effect of the Various Parameters on the Pitch Angle

The variation of σ_{θ_r} with k_d, κ, γ, and s and the manner in which this variation is affected by the system damping ratio and the relative-turbulence scale are generally similar to those of $\sigma_{a_{n,r}}$. As in the case of $\sigma_{a_{n,r}}$, there is little variation of σ_{θ_r} with k_d except for the simultaneous condition of small damping $\left(\frac{k_d}{\gamma/\kappa} \gg 1.0\right)$ and small relative-turbulence scale ($k_d s \ll 1.0$) for which σ_{θ_r} can be shown to vary in direct proportion to k_d.

There are several differences, however, between the variations of σ_{θ_r} and $\sigma_{a_{n,r}}$ with κ/γ. First of all, the parameters κ and γ are involved only in the ratio γ/κ as indicated by equation (21). Secondly, σ_{θ_r} for the nearly critically damped condition $\left(\frac{k_d}{\gamma/\kappa} \ll 1.0\right)$ and for small relative-turbulence scale $\left(\frac{\gamma s}{\kappa} \ll 1.0\right)$ can be shown to be inversely

proportional to the square root of κ/γ. For the same damping condition but for large relative-turbulence scale, σ_{θ_r} is independent of κ/γ and can be shown to be equal to unity. For very low damping ratios and for both large and small relative-turbulence scales, σ_{θ_r} can be shown to vary directly with the square root of κ/γ.

The variation of σ_{θ_r} with s is similar to that of $\sigma_{a_{n,r}}$ except for the condition of nearly critical damping and large relative-turbulence scale for which it can be shown that σ_{θ_r} is independent of s and equal to unity.

The foregoing characteristics were obtained from the following equations which are based on the same approach as used for equations (A1) and (A2). For a small relative-turbulence scale ($k_o s \ll 1.0$) and for nearly critical damping $\left(\frac{k_d}{\gamma/\kappa} \ll 1.0\right)$,

$$\sigma_{\theta_r} \approx \frac{1}{2}\left[\frac{s\gamma}{\kappa}\right]^{1/2} \tag{A3}$$

whereas for very low damping $\left(\frac{k_d}{\gamma/\kappa} \gg 1.0\right)$,

$$\sigma_{\theta_r} \approx \left[\frac{\left|\phi(k_d)\right|^2 k_d^2 s}{4\gamma/\kappa}\right]^{1/2} \tag{A4}$$

so that σ_{θ_r} and $\sigma_{a_{n,r}}$ are approximately the same. (See eq. (A1).)

For a large relative-turbulence scale ($k_o s \gg 1.0$) and for nearly critical damping,

$$\sigma_{\theta_r} \approx 1.0 \tag{A5}$$

whereas for very low damping $\left(\frac{k_d}{\gamma/\kappa} \gg 1.0\right)$,

$$\sigma_{\theta_r} \approx \left[1 + \frac{3\left|\phi(k_d)\right|^2}{4s\gamma/\kappa}\right]^{1/2} \tag{A6}$$

The second term of equation (A6) is the same as equation (A2). The unit value of the first term accounts for the area under the product of the power spectrum and the transfer-function modulus squared over the range of frequencies from zero to a frequency at which the value of the power spectrum is extremely small, the value of the transfer function-modulus over this frequency range being unity. (See fig. 7(a).)

The characteristics indicated by equations (A3) to (A6) for variations of σ_{θ_r} with γ/κ can be observed in figure 6. As in the presentation of $\sigma_{a_{n,r}}$, the reciprocal of γ/κ is used. The sample curves presented in figure 6(a) for $s = 50$ indicate differences in the trends of σ_{θ_r} with κ/γ for different frequencies. The sample curves presensented in figure 6(b) for $s = 2,000$ indicate similar trends of σ_{θ_r} with κ/γ for different frequencies. The trends of σ_{θ_r} with k_d, γ/κ, and s are summarized in table II.

REFERENCES

1. Donely, Philip: Summary of Information Relating to Gust Loads on Airplanes. NACA Rep. 997, 1950. (Supersedes NACA TN 1976.)

2. Wiener, Norbert: Generalized Harmonic Analysis. Acta Mathematica, vol. 55, 1930, pp. 117-258.

3. Clementson, Gerhardt C.: An Investigation of the Power Spectral Density of Atmospheric Turbulence. Ph.D. Thesis, M.I.T., 1950.

4. Press, Harry, and Mazelsky, Bernard: A Study of the Application of Power-Spectral Methods of Generalized Harmonic Analysis to Gust Loads on Airplanes. NACA Rep. 1172, 1954. (Supersedes NACA TN 2853.)

5. Press, Harry, and Houbolt, John C.: Some Applications of Generalized Harmonic Analysis to Gust Loads on Airplanes. Jour. Aero. Sci., vol. 22, no. 1, Jan. 1955, pp. 17-26, 60.

6. Zbrožek, J. K.: A Study of the Longitudinal Response of Aircraft to Turbulent Air. Rep. No. Aero. 2530, British R.A.E., Jan. 1955.

7. Diederich, Franklin W.: The Response of an Airplane to Random Atmospheric Disturbances. NACA TN 3910, 1957.

8. Liepmann, H. W.: On the Application of Statistical Concepts to the Buffeting Problem. Jour. Aero. Sci., vol. 19, no. 12, Dec. 1952. pp. 793-800, 822.

9. Anon: Fundamentals of Design of Piloted Aircraft Flight Control Systems. Vol. II - Dynamics of the Airframe. Rep. AE-61-4, Bur. Aero., Feb. 1953.

10. Fung, Y. C.: Statistical Aspects of Dynamic Loads. Jour. Aero. Sci., vol. 20, no. 5, May 1953, pp. 317-330.

11. Diederich, Franklin W., and Foss, Kenneth A.: Charts and Approximate Formulas for the Estimation of Aeroelastic Effects on the Loading of Swept and Unswept Wings. NACA Rep. 1140, 1953. (Supersedes NACA TN 2608.)

TABLE I.- ROOT-MEAN-SQUARE PITCHING-ACCELERATION RATIO, $\sigma_{\ddot{\theta}_r}$

K	k_d \ s	50				100				200				500				2,000			
		1	2	5	10	1	2	5	10	1	2	5	10	1	2	5	10	1	2	5	10
40	0	-----	-----	0.203	0.119	-----	-----	0.146	0.0849	-----	-----	-----	-----	-----	-----	0.0660	0.0381	-----	-----	0.0330	0.0190
	.01	0.521	0.368	.203	.119	0.415	0.277	.146	.0849	0.309	0.200	0.104	0.0601	0.200	0.128	.0660	.0381	0.100	0.0639	.0330	.0190
	.02	.530	.369	.203	.119	.418	.276	.146	.0848	.309	.200	.104	.0601	.199	.127	.0659	.0380	.0996	.0637	.0330	.0190
	.05	.556	.371	.202	.119	.419	.274	.145	.0846	.302	.196	.103	.0600	.192	.125	.0655	.0379	.0962	.0624	.0328	.0190
	.10	.548	.364	.199	.118	.397	.263	.143	.0839	.283	.187	.101	.0593	.179	.119	.0641	.0376	.0895	.0594	.0321	.0188
	.20	.490	.333	.189	.113	.349	.237	.134	.0815	.247	.168	.095	.0577	.157	.106	.0602	.0365	.0783	.0532	.0301	.0182
100	0	-----	-----	0.368	0.238	-----	-----	0.277	0.173	-----	-----	-----	-----	-----	-----	0.128	0.0781	-----	-----	0.0639	0.0391
	.01	0.721	0.571	.368	.238	0.639	0.466	.277	.173	0.509	0.352	0.200	0.123	0.341	0.229	.128	.0780	0.173	0.115	.0639	.0390
	.02	.790	.588	.369	.238	.678	.473	.276	.172	.520	.352	.200	.123	.339	.227	.127	.0779	.171	.114	.0637	.0390
	.05	.914	.629	.371	.237	.700	.476	.274	.171	.507	.344	.196	.122	.323	.219	.125	.0773	.162	.110	.0624	.0386
	.10	.902	.621	.364	.233	.654	.450	.263	.167	.465	.320	.187	.119	.295	.203	.119	.0762	.148	.102	.0594	.0376
	.20	.793	.553	.333	.218	.566	.394	.237	.156	.401	.279	.168	.110	.254	.176	.106	.0697	.127	.0882	.0532	.0349
250	0	-----	-----	-----	0.415	-----	-----	0.462	0.317	-----	-----	-----	-----	-----	-----	0.229	0.148	-----	-----	0.115	0.0742
	.01	0.920	0.768	0.571	0.416	0.920	0.700	.466	.317	0.799	0.570	0.352	0.231	0.558	0.385	.229	.148	0.286	0.196	.115	.0742
	.02	1.16	.866	.588	.418	1.07	.759	.473	.318	.847	.587	.352	.231	.537	.384	.227	.147	.281	.193	.114	.0739
	.05	1.47	1.03	.629	.424	1.14	.789	.476	.315	.823	.571	.344	.227	.524	.364	.219	.144	.262	.182	.110	.0721
	.10	1.45	1.01	.621	.417	1.05	.735	.450	.302	.749	.523	.320	.213	.474	.332	.203	.136	.237	.166	.102	.0681
	.20	1.27	.892	.553	.379	.904	.655	.394	.270	.640	.450	.279	.191	.405	.285	.176	.121	.203	.142	.0882	.0604
1,000	0	-----	-----	0.774	0.689	-----	-----	0.738	-----	-----	-----	-----	-----	-----	-----	0.478	0.339	-----	-----	0.255	0.174
	.01	1.39	1.11	.869	.721	1.63	1.21	.843	0.639	1.37	1.12	0.717	0.509	1.14	0.800	.496	.341	0.587	0.411	.254	.173
	.02	2.17	1.37	1.05	.790	2.13	1.52	.960	.678	1.72	1.21	.753	.520	1.14	.798	.494	.339	.573	.402	.249	.171
	.05	2.98	2.10	1.31	.914	2.30	1.62	1.01	.700	1.67	1.17	.732	.507	1.06	.748	.467	.323	.532	.374	.234	.162
	.10	2.93	2.06	1.29	.902	2.12	1.50	.938	.654	1.51	1.06	.668	.465	.957	.675	.423	.295	.478	.337	.212	.147
	.20	2.55	1.80	1.13	.793	1.82	1.28	.807	.566	1.29	.908	.572	.401	.814	.575	.362	.254	.407	.287	.181	.127
20,000	0	-----	-----	0.869	0.865	-----	-----	0.910	0.900	-----	-----	-----	-----	-----	-----	0.927	0.881	-----	-----	0.818	-----
	.01	5.19	3.72	2.43	1.81	6.88	4.88	3.12	2.24	7.00	4.95	3.13	2.22	5.14	3.63	2.29	1.62	2.65	1.87	1.18	0.834
	.02	9.44	6.68	4.25	3.02	9.61	6.80	4.30	3.04	7.76	5.48	3.47	2.43	5.12	3.62	2.29	1.61	2.58	1.82	1.15	.815
	.05	13.4	9.45	5.97	4.22	10.3	7.31	4.62	3.26	7.49	5.30	3.35	2.36	4.77	3.37	2.13	1.51	2.39	1.69	1.07	.754
	.10	13.1	9.29	5.87	4.15	9.52	6.73	4.25	3.01	6.77	4.79	3.03	2.14	4.29	3.03	1.92	1.35	2.15	1.52	.959	.678
	.20	11.4	8.08	5.11	3.61	8.14	5.75	3.64	2.57	5.76	4.07	2.58	1.82	3.65	2.58	1.63	1.15	1.83	1.29	.815	.576

TABLE II.- SUMMARY OF EFFECTS OF CHANGES IN k_d, κ, γ, AND s ON $\sigma_{a_{n,r}}$ AND σ_{θ_r}

Damping ratio	Relative-turbulence scale	Equation	Variation of σ with -		
			s	k_d	κ/γ
$\sigma_{a_{n,r}}$					
Nearly unity, $\frac{k_d}{\gamma\kappa} \ll 1.0$	Small, $k_o s = s\gamma/\kappa \ll 1.0$	----	$\propto s^{1/2}$	Independent	Increases with κ/γ and increases with γ for given value of κ/γ
	Large, $k_o s = s\gamma/\kappa \gg 1.0$	----	Decreases with s		
Less than 0.1, $\frac{k_d}{\gamma/\kappa} \gg 1.0$	Small, $k_o s = k_d s \ll 1.0$	(A1)	$\propto s^{1/2}$	$\propto k_d$	$\propto (\kappa/\gamma)^{1/2}$ and independent of γ for given value of κ/γ
	Large, $k_o s = k_d s \gg 1.0$	(A2)	$\propto s^{-1/2}$	[1]Independent	
σ_{θ_r}					
Nearly unity, $\frac{k_d}{\gamma/\kappa} \ll 1.0$	Small, $k_o s = s\gamma/\kappa \ll 1.0$	(A3)	$\propto s^{1/2}$	Independent	$\propto (\kappa/\gamma)^{-1/2}$
	Large, $k_o s = s\gamma/\kappa \gg 1.0$	(A5)	≈ 1.0	[1]Independent and equals 1.0	≈ 1.0
Less than 0.1, $\frac{k_d}{\gamma/\kappa} \gg 1.0$	Small, $k_o s = k_d s \ll 1.0$	(A4)	$\propto s^{1/2}$	$\propto k_d$	$\propto (\kappa/\gamma)^{1/2}$
	Large, $k_o s = k_d s \gg 1.0$	(A6)	$\propto s^{-1/2}$	[1]Independent	

[1]Decreases somewhat with k_d at higher values of k_d, due to unsteady lift.

TABLE III.- CHARACTERISTICS OF BASIC AIRPLANE

$C_{L_{\alpha,w}}$, per radian	5.6
$C_{L_{\alpha,t}}$, (based on tail area) per radian	4.2
$\bar{c}$, ft	6.72
$\bar{c}_t$, ft	3.08
l_w, ft	0.229
l_t, ft	-14.9
r, ft	6.72
S, sq ft	237
S_t, sq ft	43.5
U, ft/sec	660
W, lb	10,936
$d\epsilon/d\alpha$	0.5
ρ, slugs/cu ft	0.002209

TABLE IV.- AIRPLANE CHARACTERISTICS FOR CHANGE IN CENTER OF GRAVITY

[s = 297]

Item	Center-of-gravity position	
	Forward	Rearward
l_w, ft	0.229	0.672
r, ft	6.72	6.82
W, lb	10,936	10,610
L, ft	1,000	1,000
κ	138	134
γ	2.01	1.98
k_d	0.0283	0.0178
$\sigma_{a_{n,r}}$	0.390	0.407
$(a_{n,s})_a/(a_{n,s})_f$	1.03	
$(\sigma_{a_n})_a/(\sigma_{a_n})_f$	1.075	

TABLE V.- AIRPLANE CHARACTERISTICS FOR CHANGE IN ALTITUDE

[s = 297]

Item	Altitude, h, ft	
	0	40,000
ρ, slug/cu ft	0.002378	0.000582
κ	123	501
γ	2.01	2.01
k_d	0.0276	0.0152
$\sigma_{a_{n,r}}$	0.365	0.730
$(a_{n,s})_{40}/(a_{n,s})_{sl}$	0.494	
$(\sigma_{a_n})_{40}/(\sigma_{a_n})_{sl}$	0.99	

TABLE VI.- AIRPLANE CHARACTERISTICS FOR CHANGE IN SCALE

[$a_{n,s}$, κ, γ, and k_d constant; same as for basic airplane, table IV, center of gravity forward]

Item	Basic scale	Twice basic scale
$\bar{c}$, ft	6.72	13.44
s	297	149
$\sigma_{a_{n,r}}$	0.390	0.527
$(\sigma_{a_n})_2/\sigma_{a_n}$	1.35	

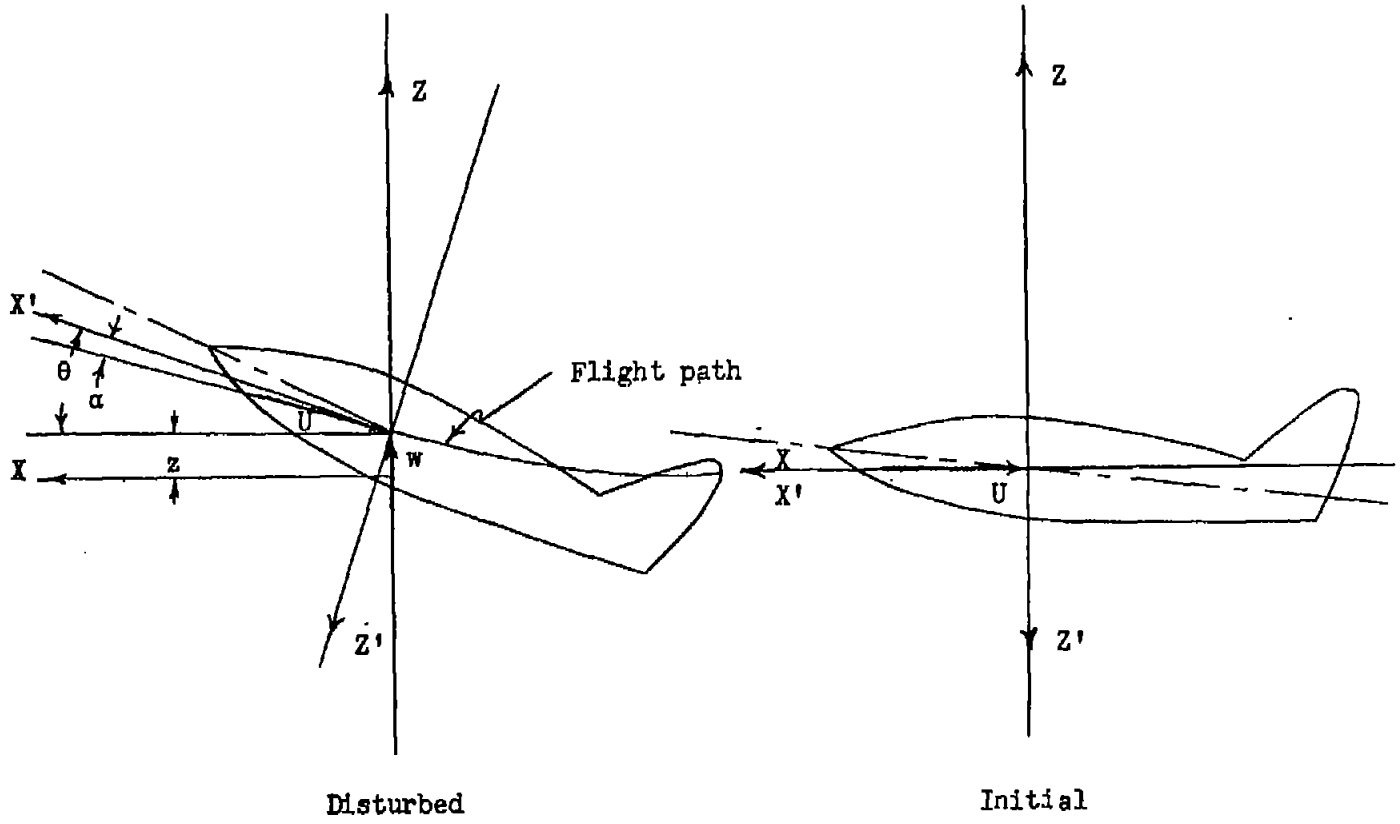

Figure 1.- Stability and space axes, positive directions shown.

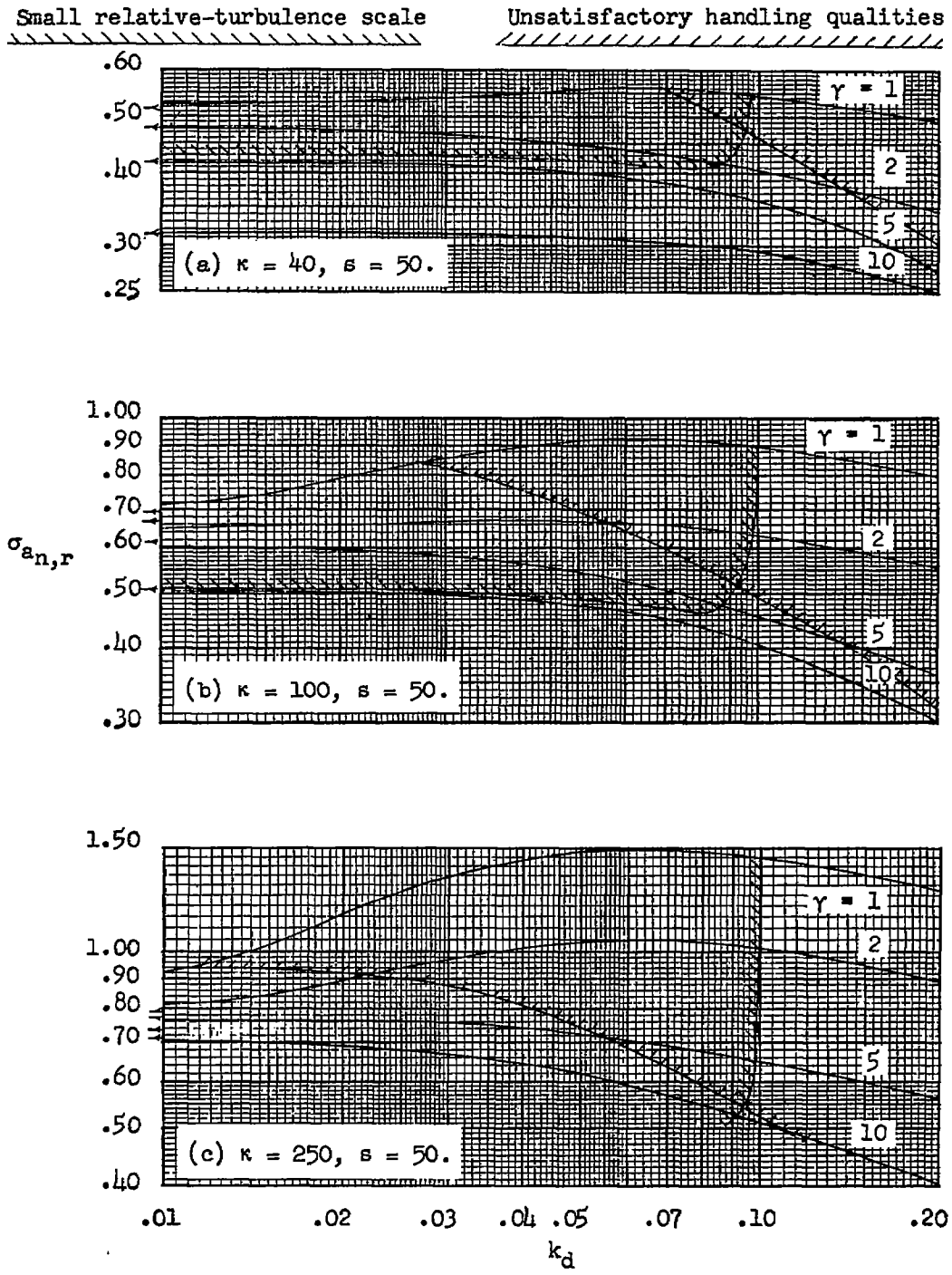

Figure 2.- Variation of root-mean-square acceleration ratio with damped-natural-frequency parameter. (Arrows indicate values for $k_d = 0$.)

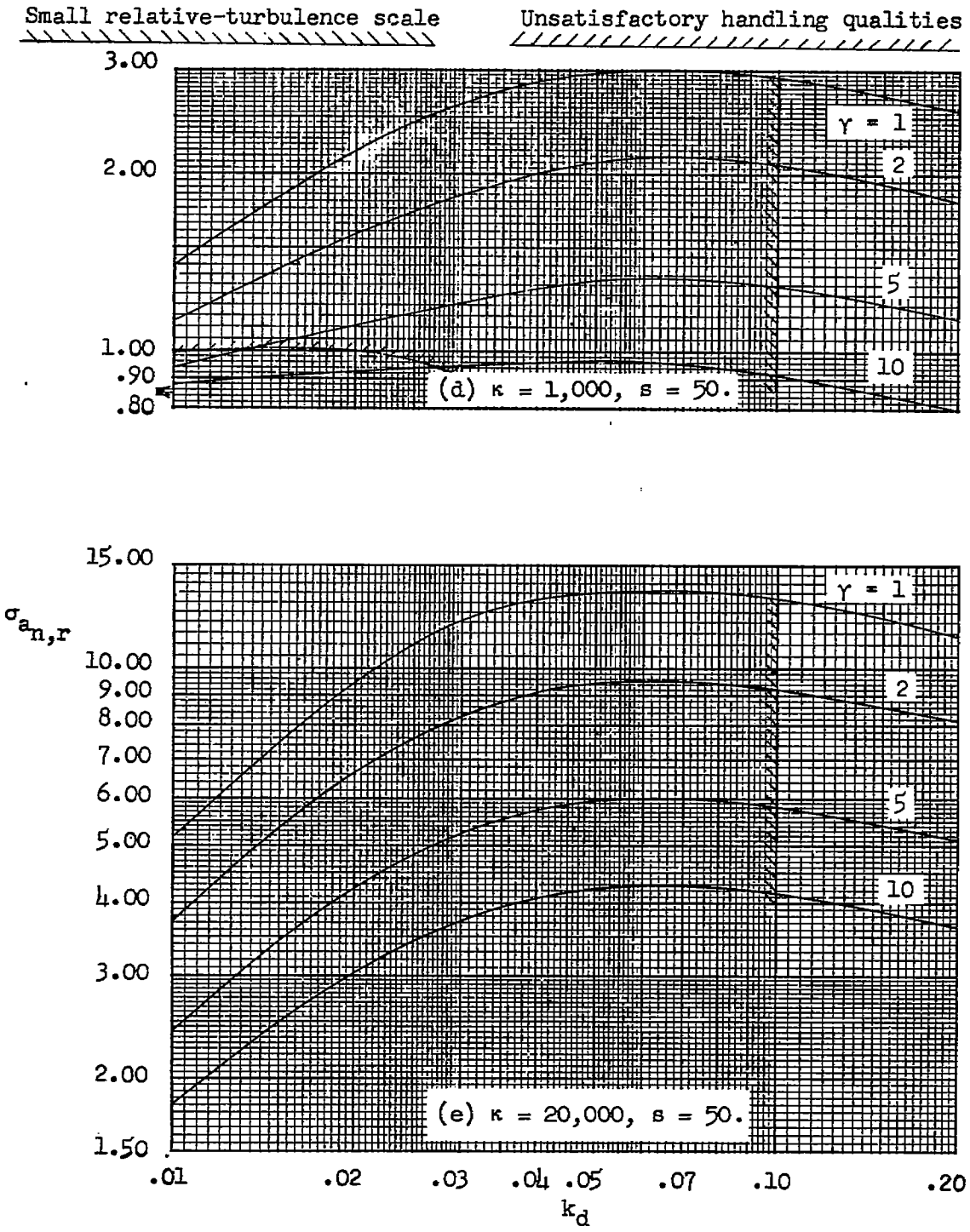

Figure 2.- Continued.

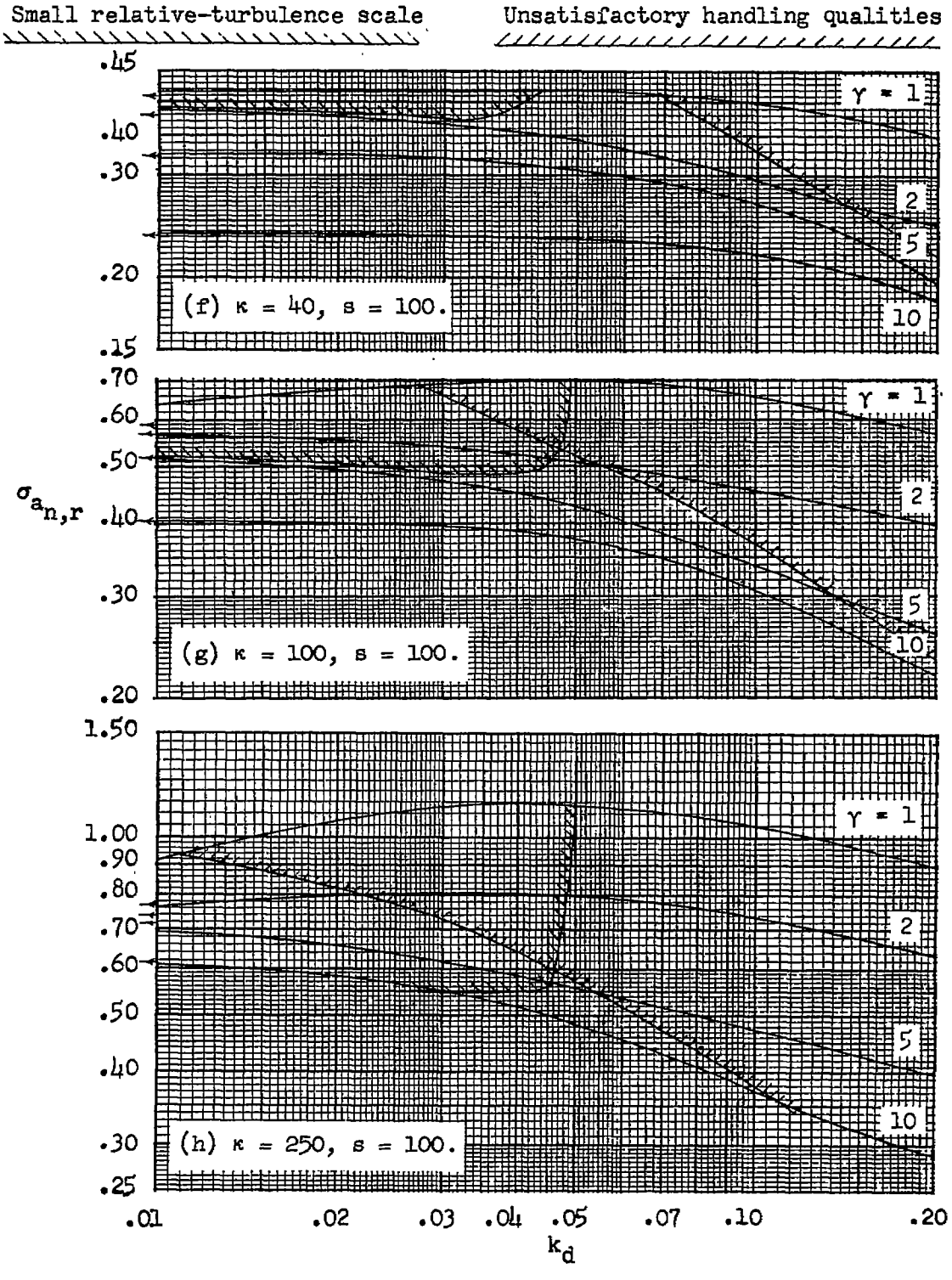

Figure 2.- Continued.

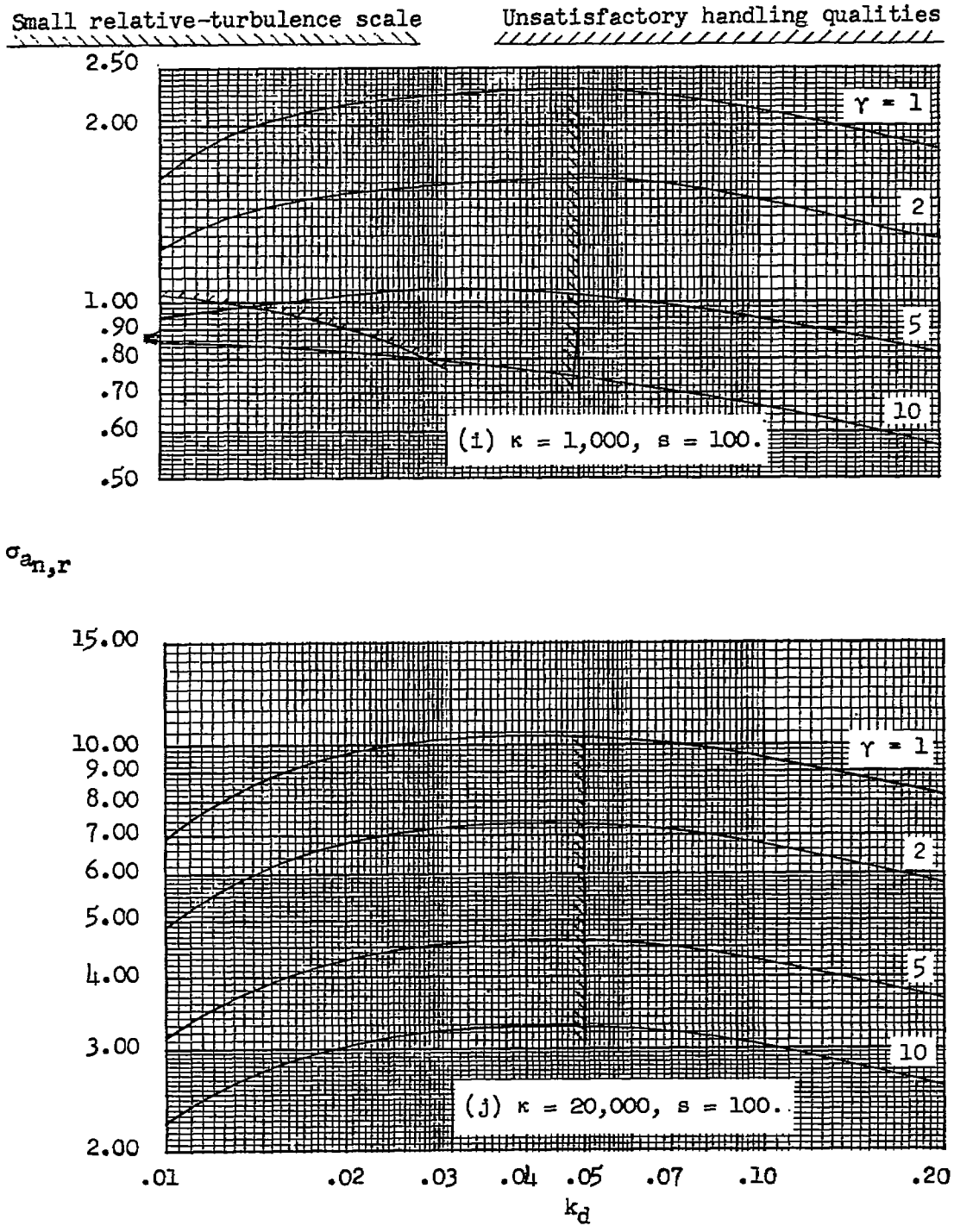

Figure 2.- Continued.

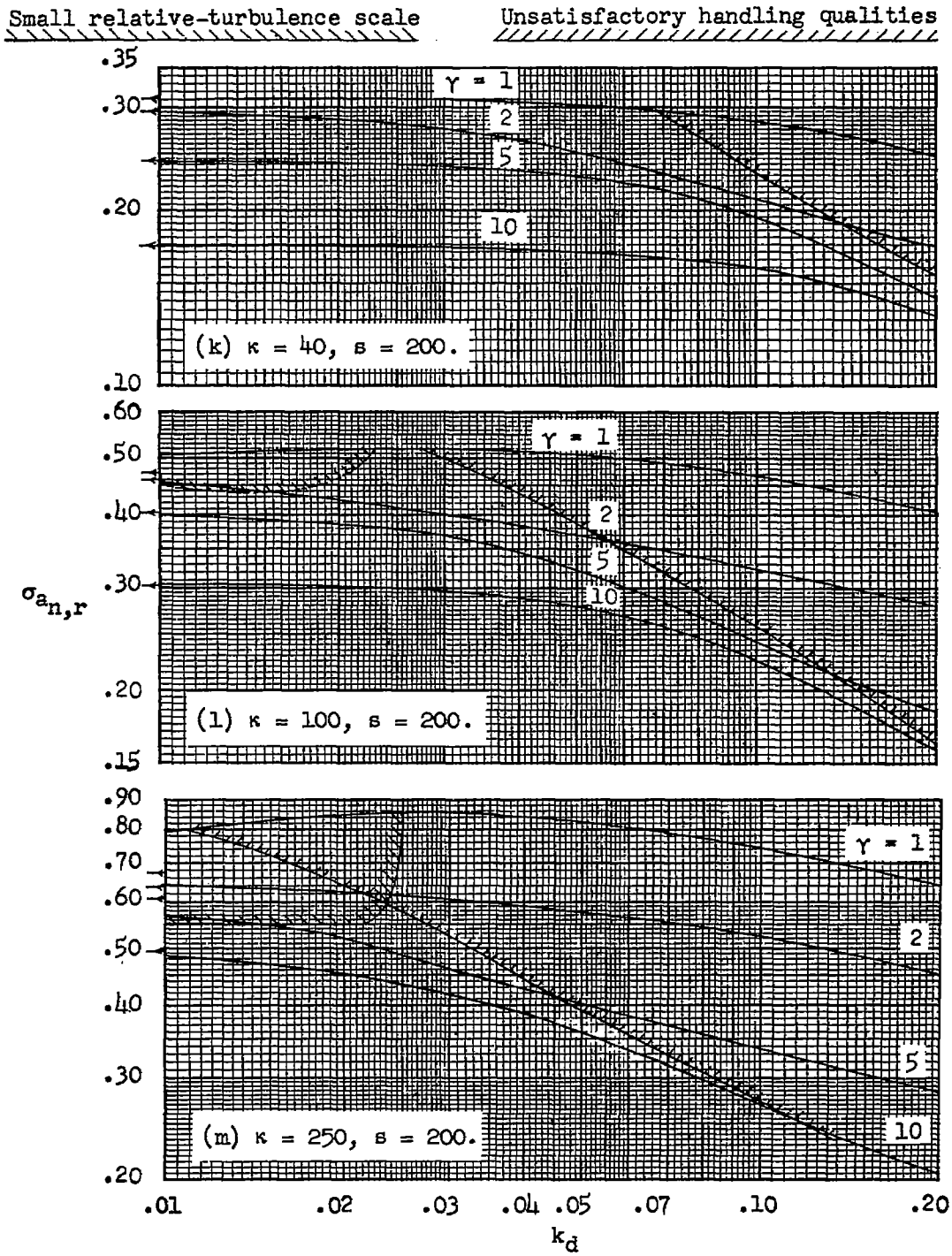

Figure 2.- Continued.

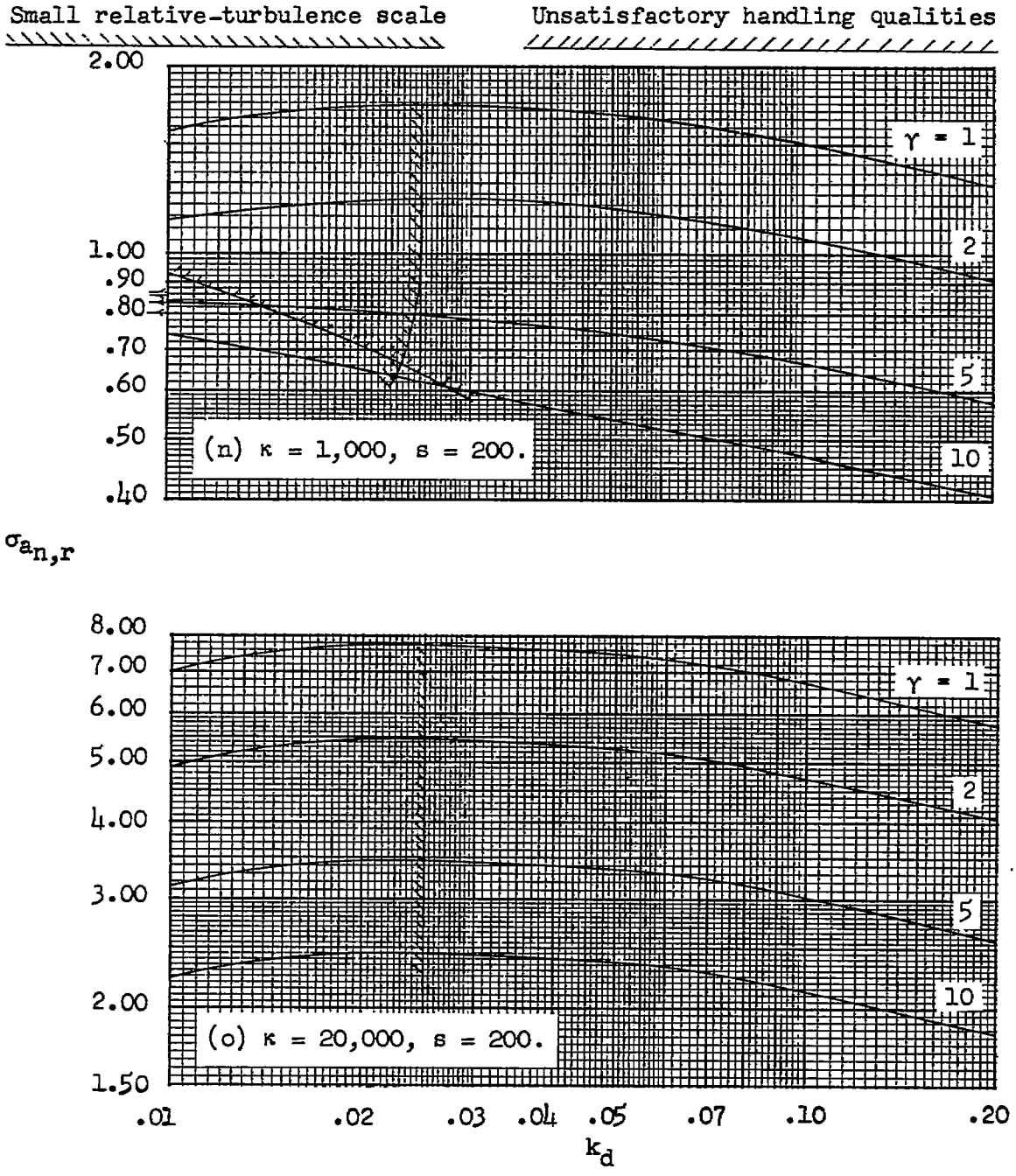

Figure 2.- Continued.

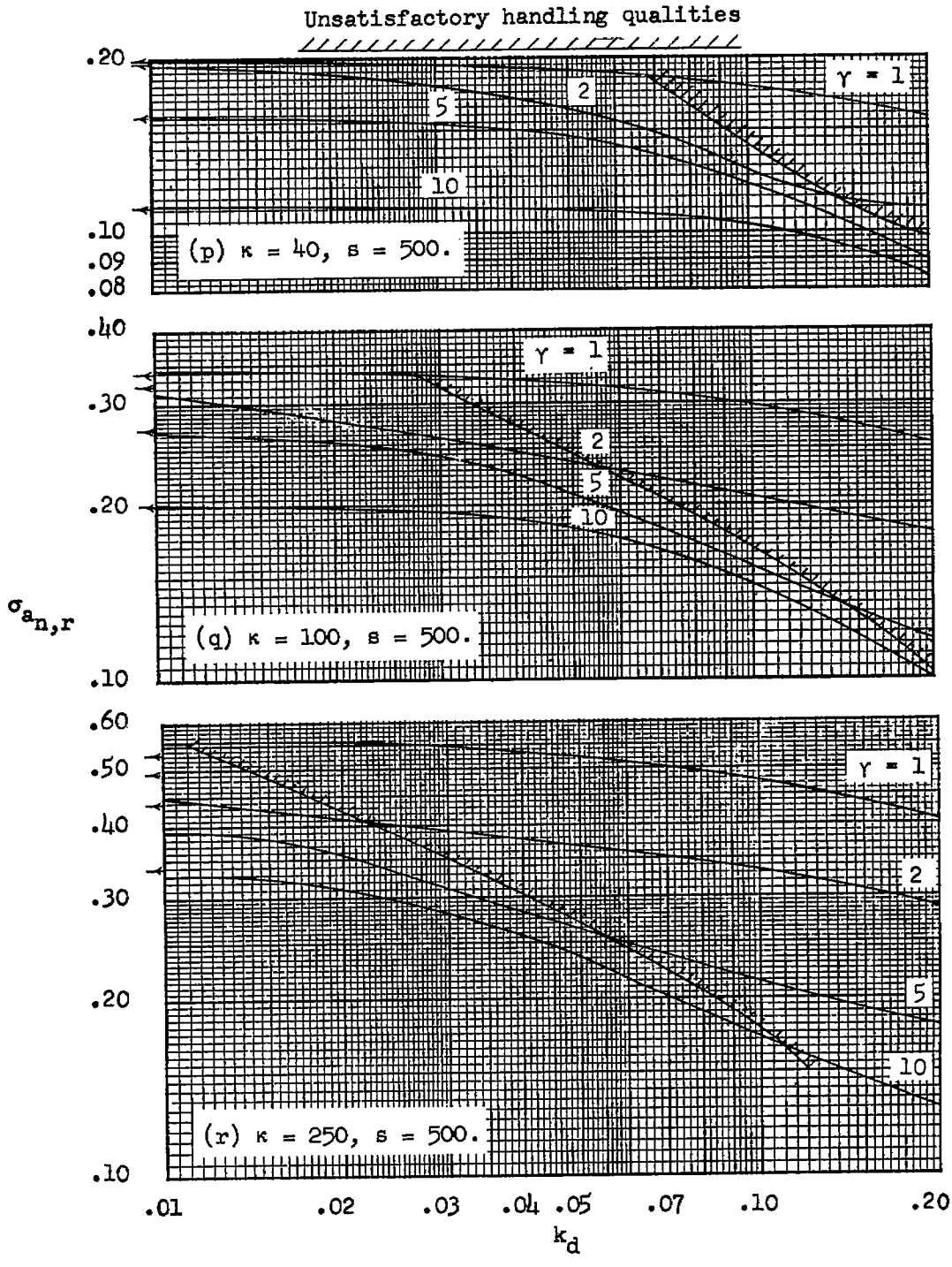

Figure 2.- Continued. (Large relative-turbulence scale.)

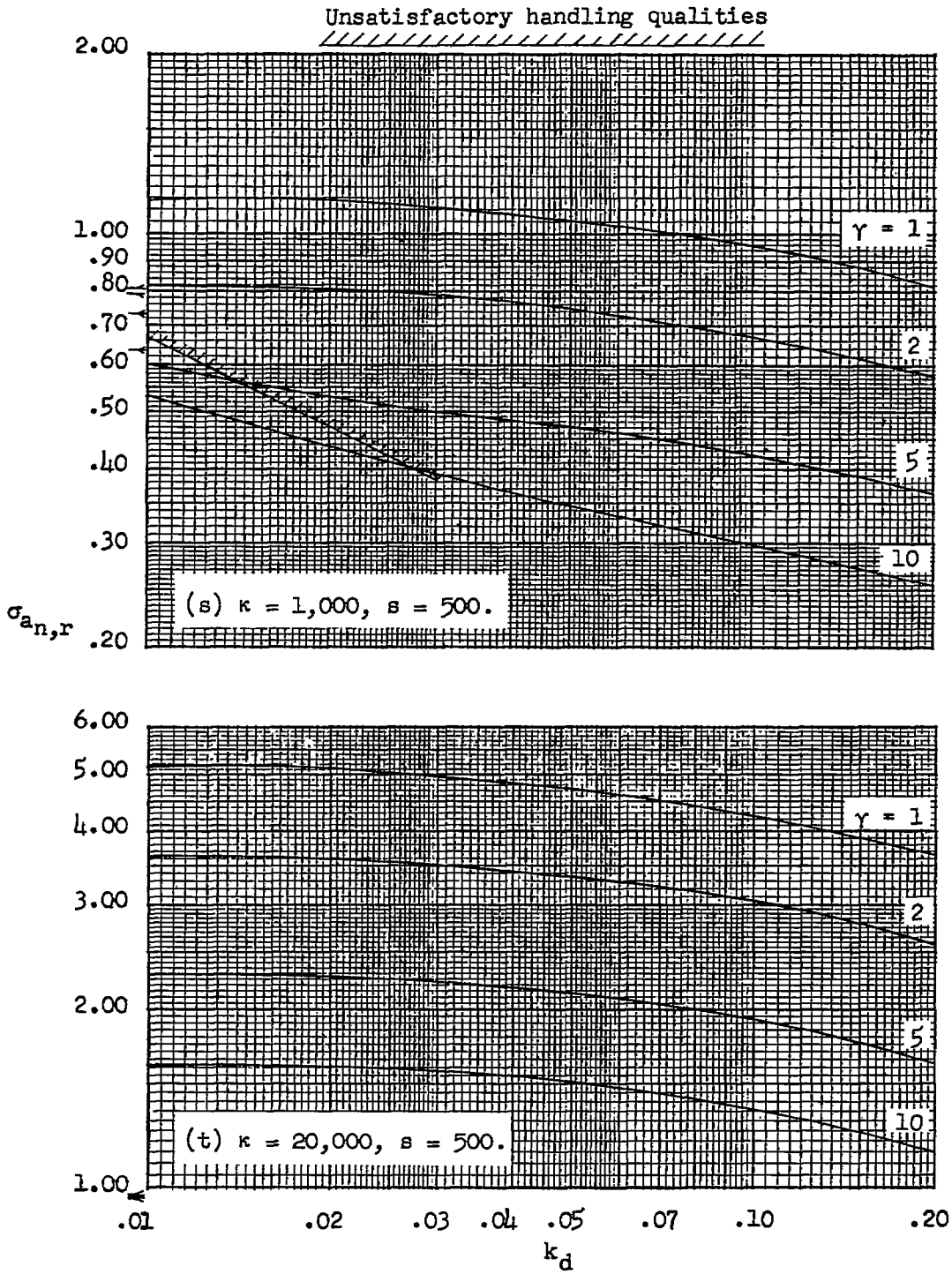

Figure 2.- Continued. (Large relative-turbulence scale.)

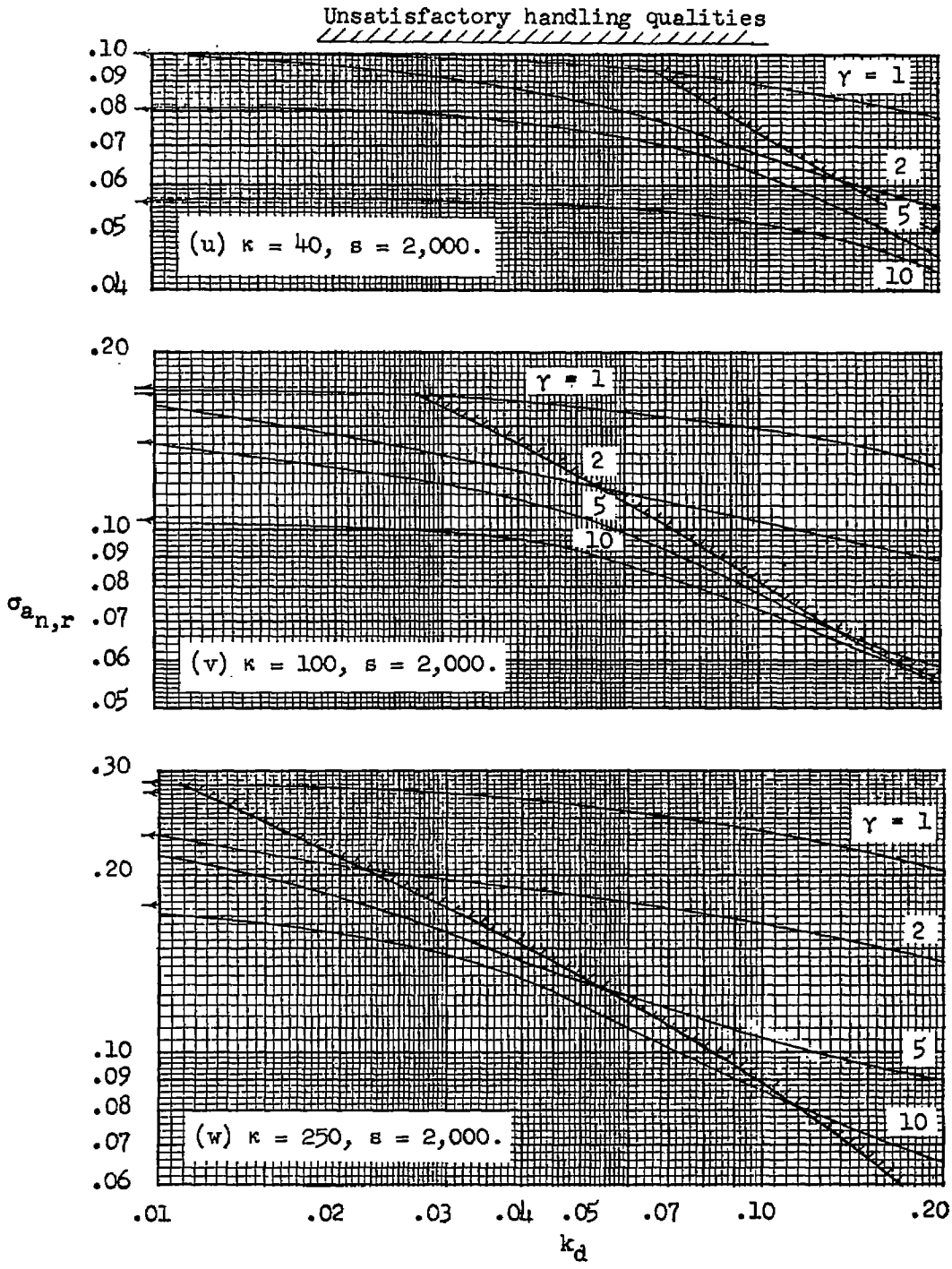

Figure 2.- Continued. (Large relative-turbulence scale.)

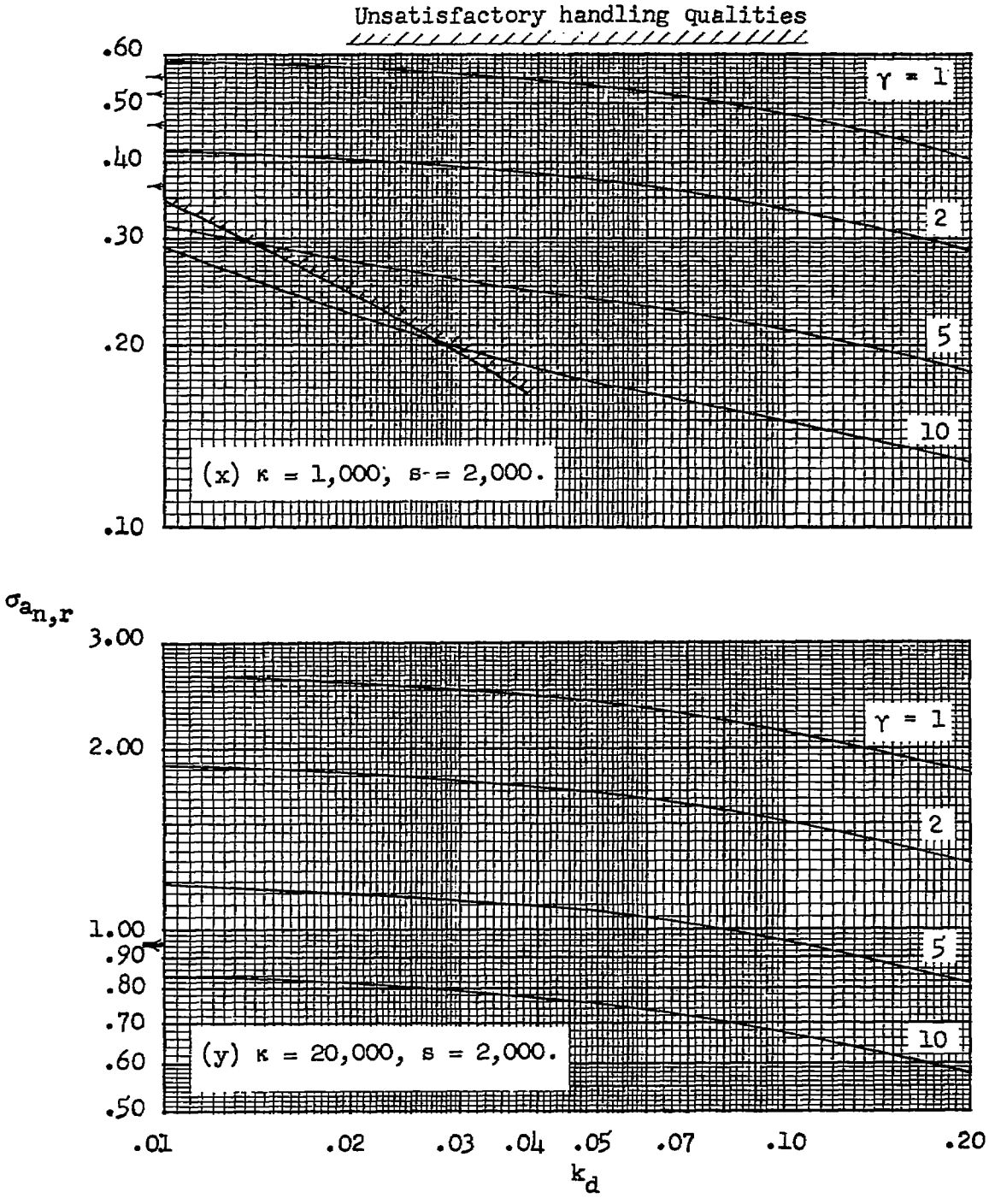

Figure 2.- Concluded. (Large relative-turbulence scale.)

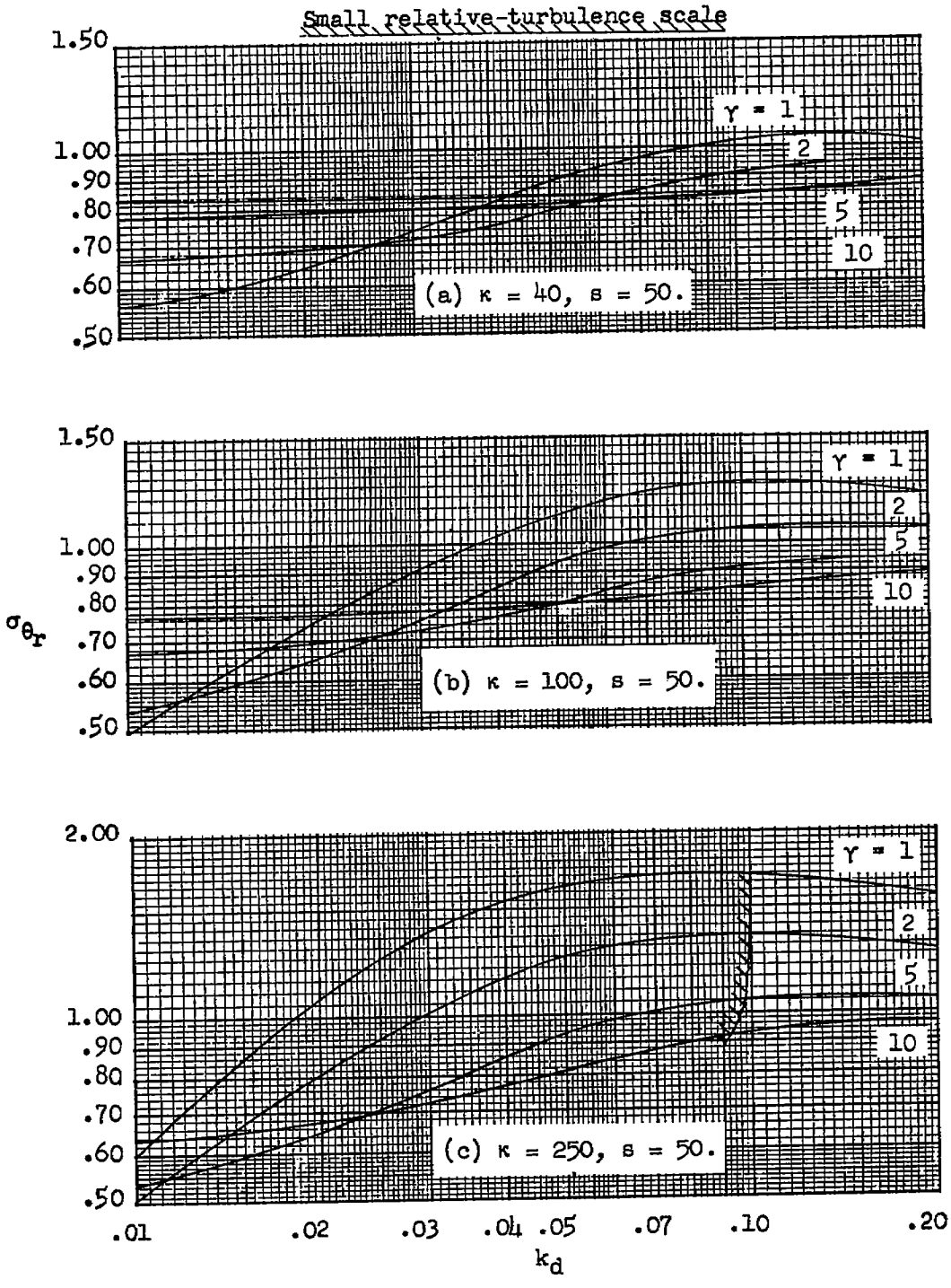

Figure 3.- Variation of root-mean-square pitch-angle ratio with damped-natural-frequency parameter.

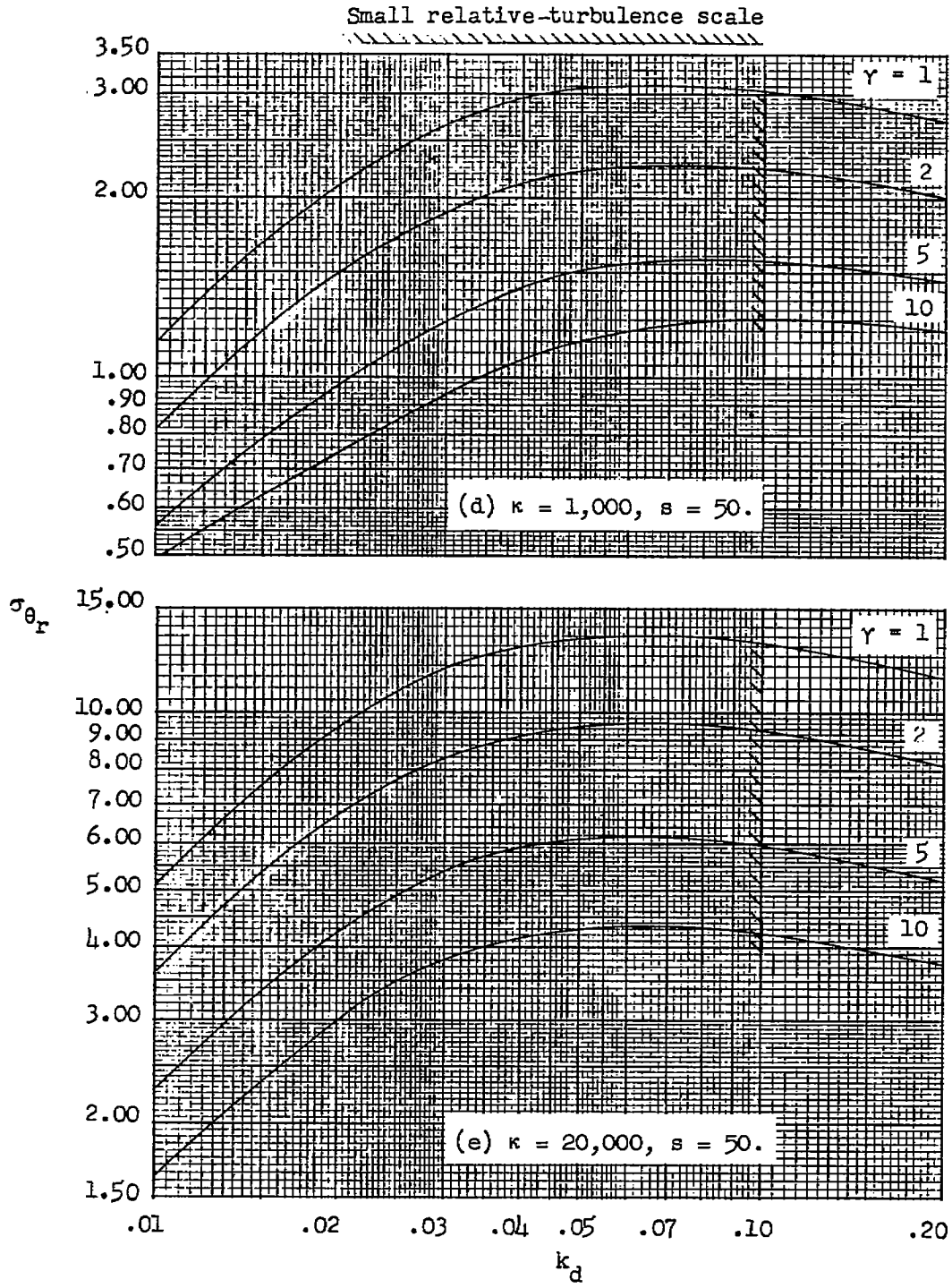

Figure 3.- Continued.

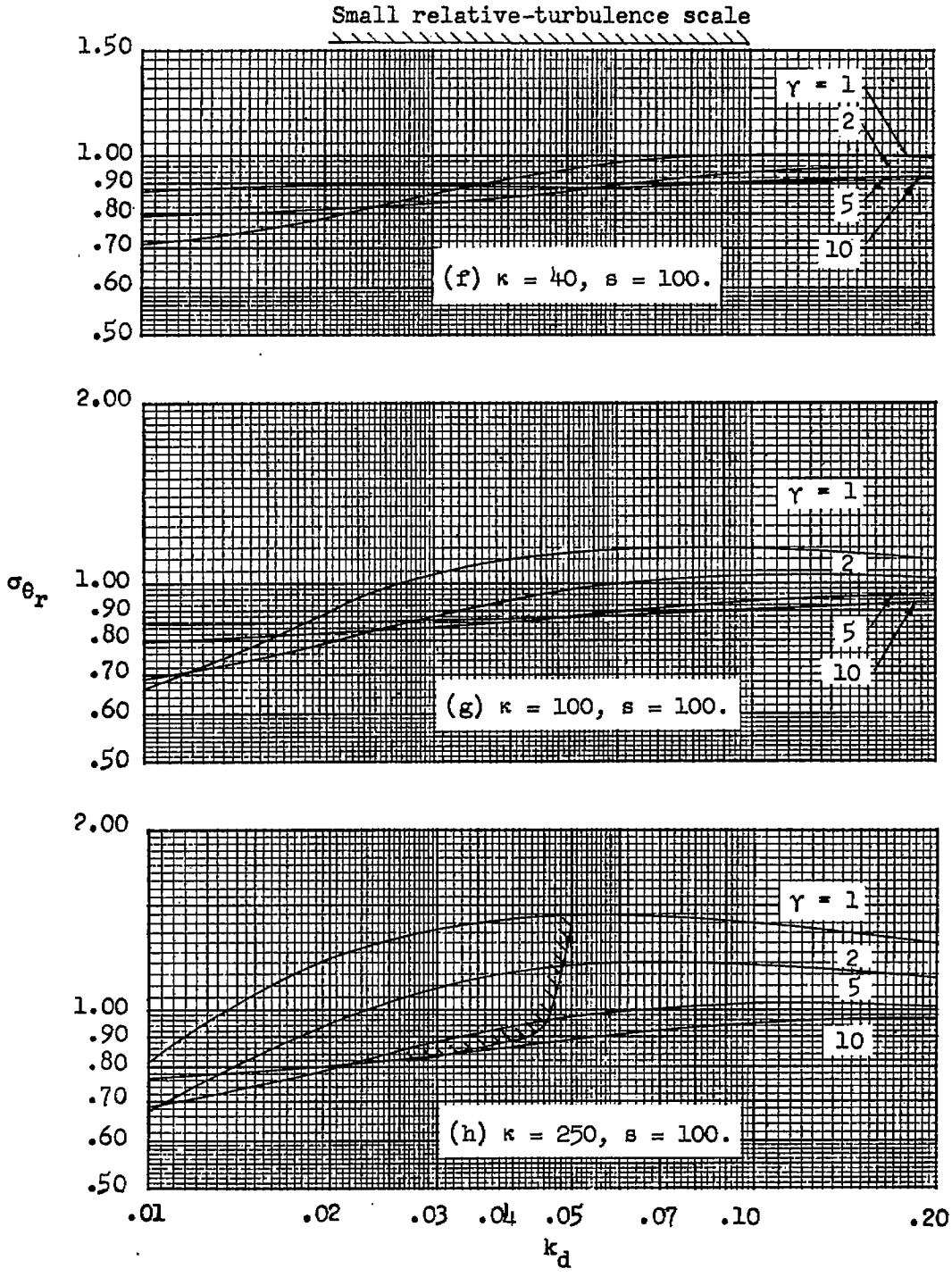

Figure 3.- Continued.

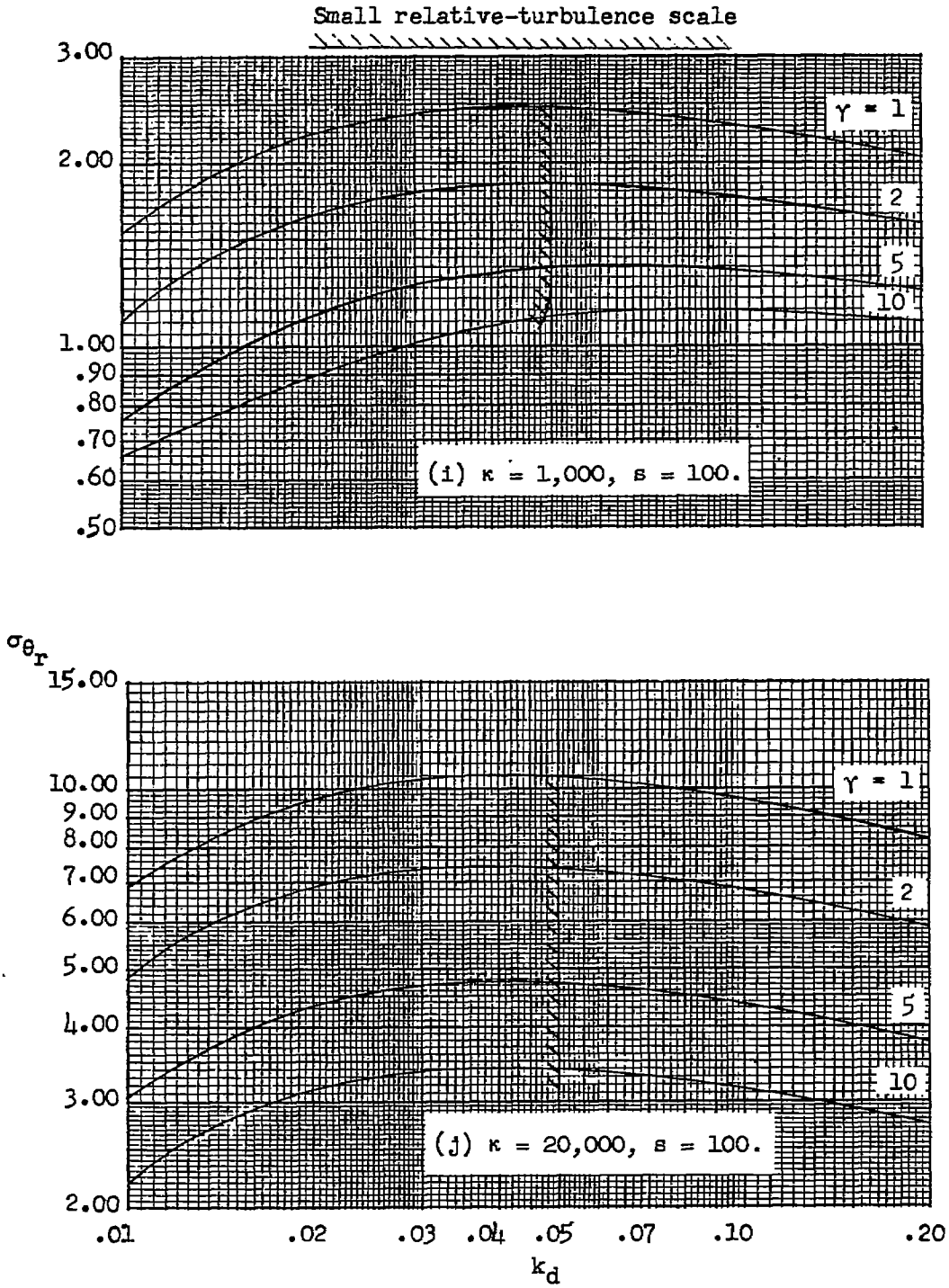

Figure 3.- Continued.

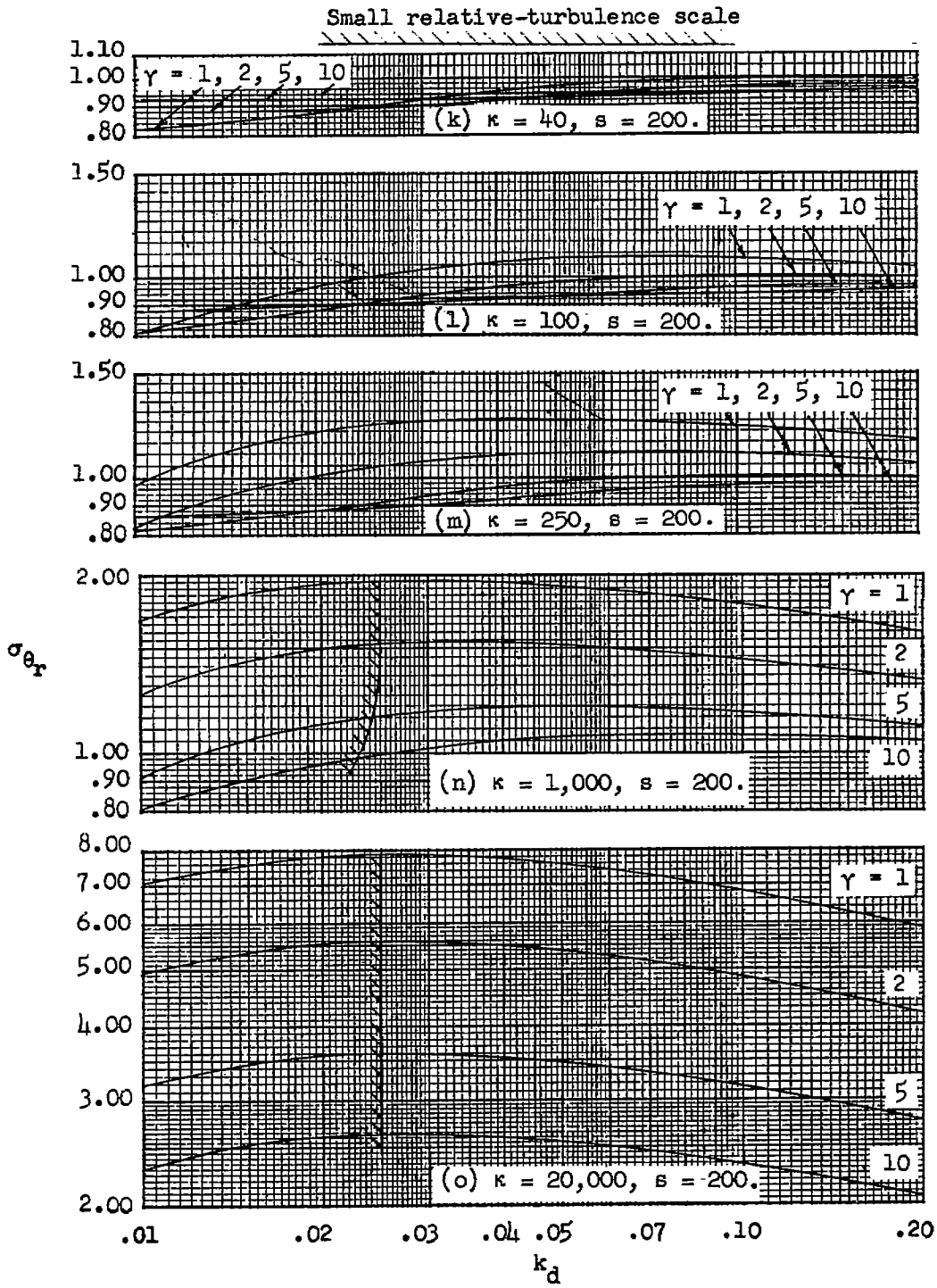

Figure 3.- Continued.

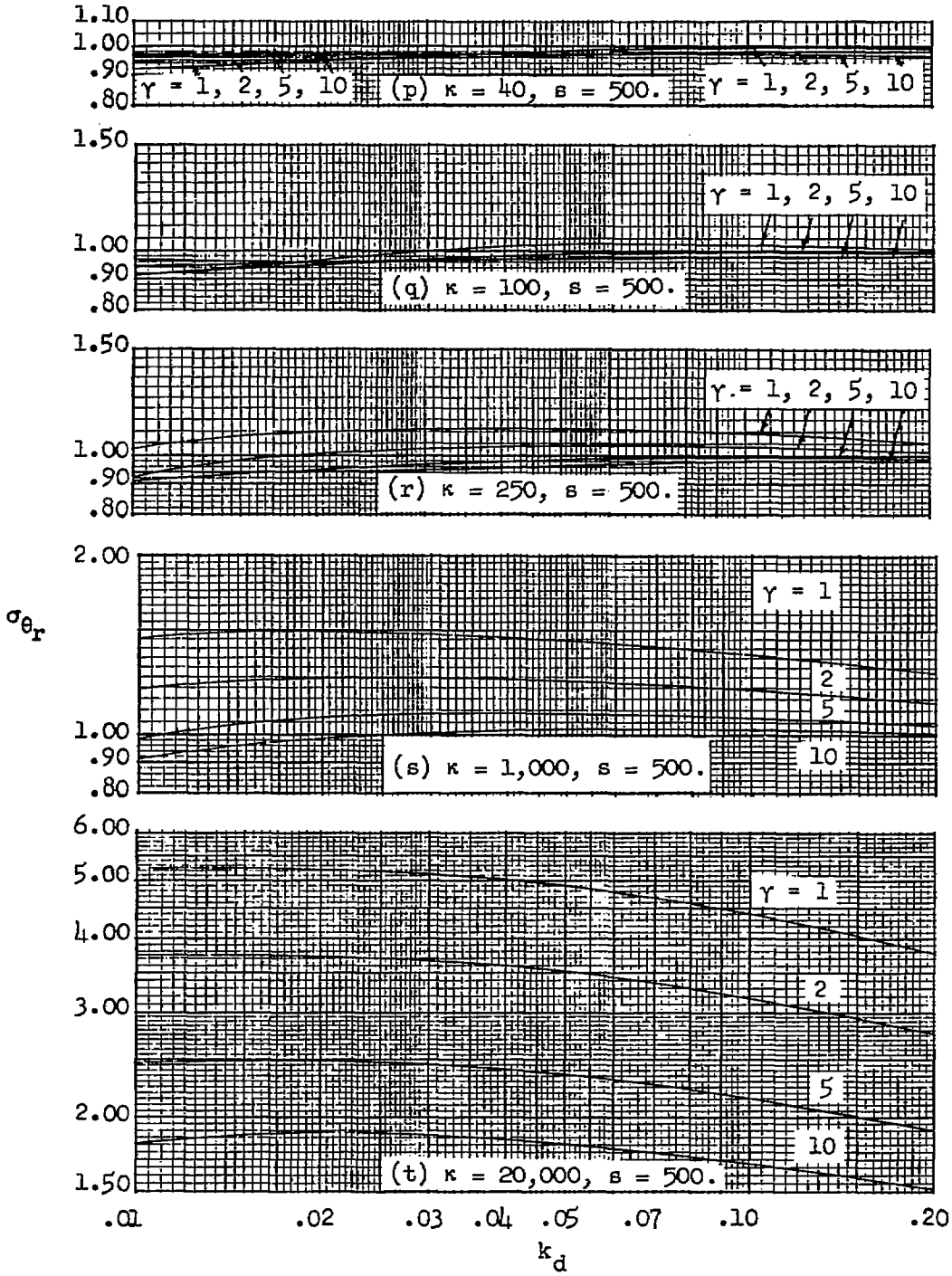

Figure 3.- Continued. (Large relative-turbulence scale.)

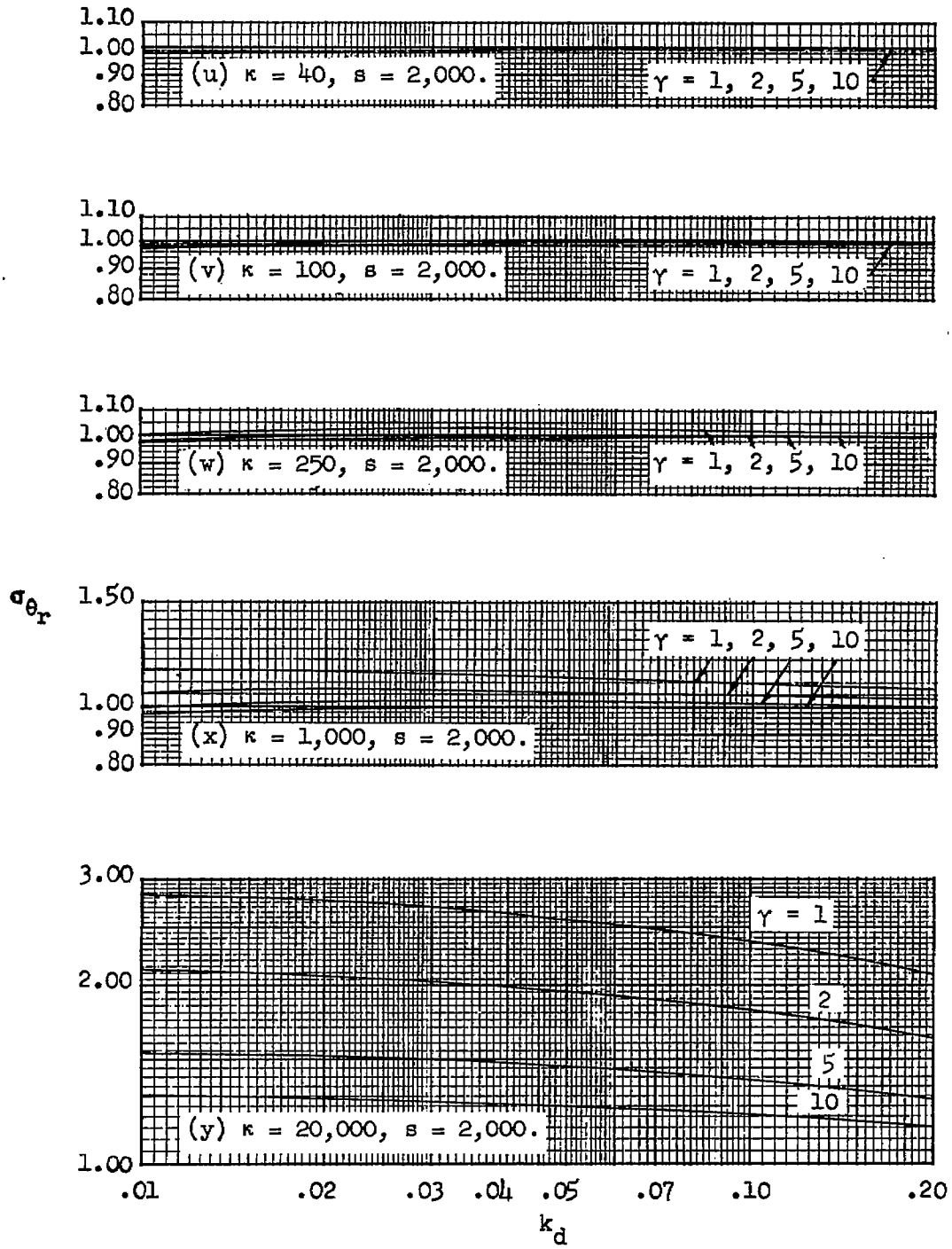

Figure 3.- Concluded. (Large relative-turbulence scale.)

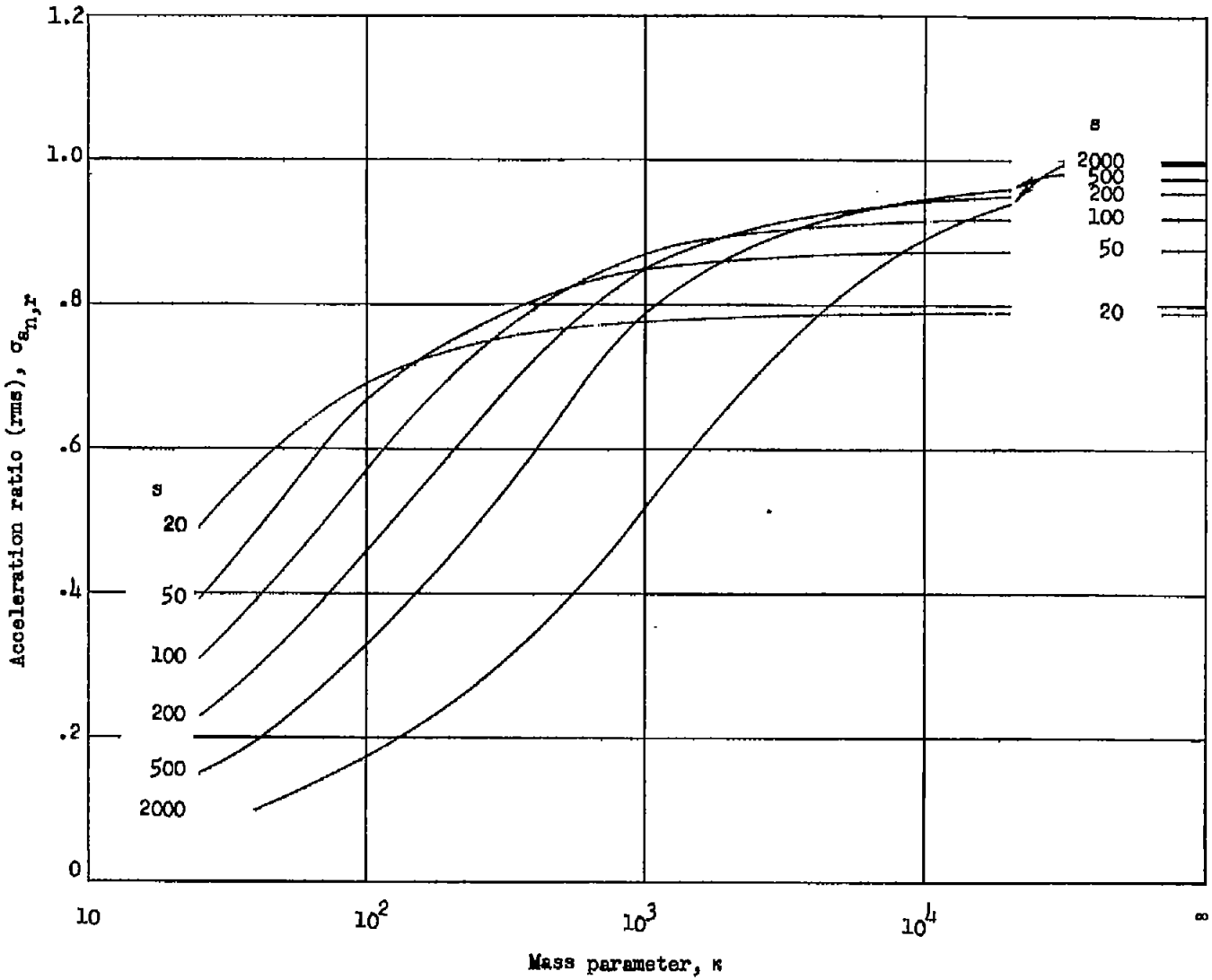

Figure 4.- Variation of root-mean-square vertical-acceleration ratio with mass parameter for nonpitching airplane. $k_d = 0$; $\gamma = 2$.

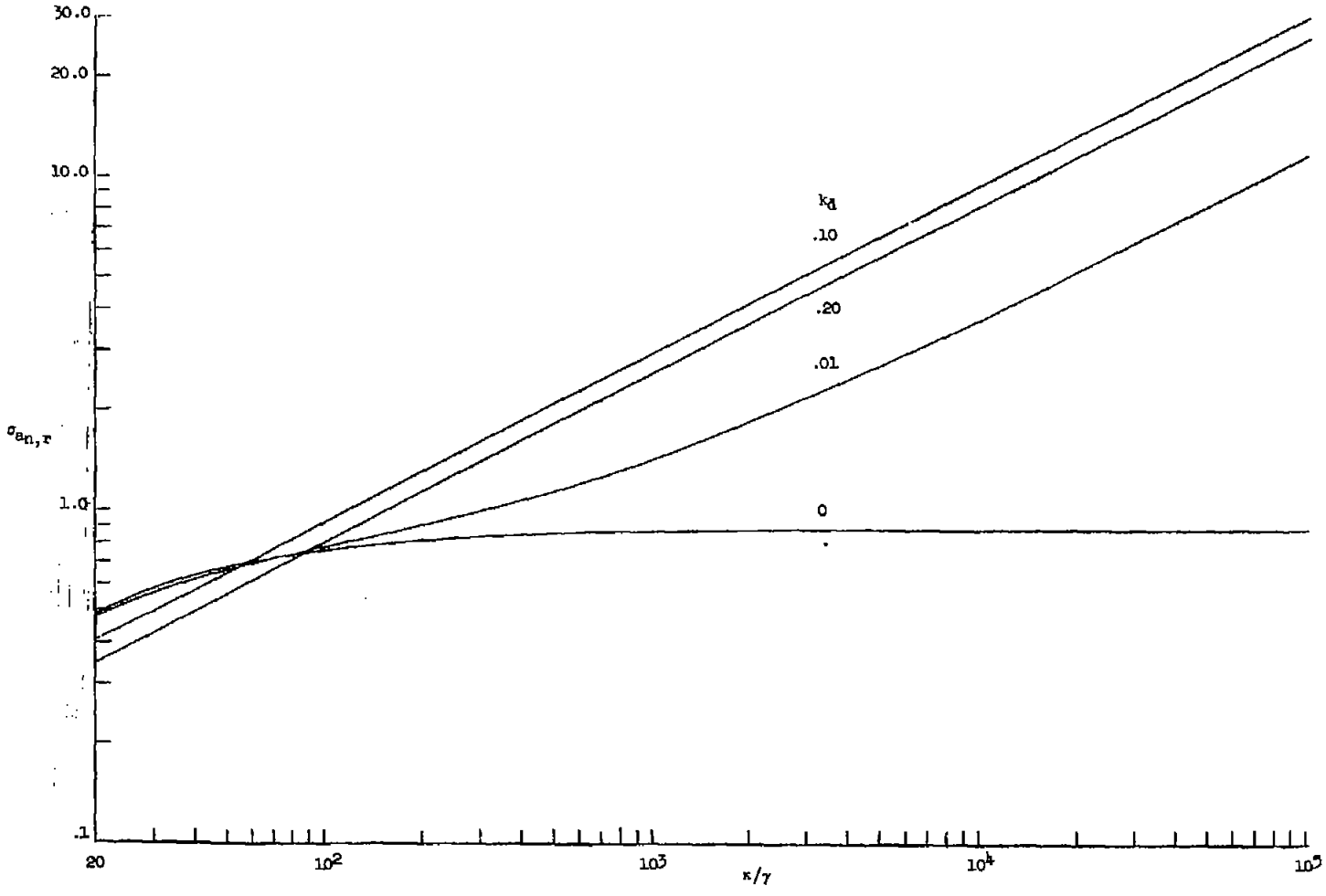

(a) $s = 50$; $\gamma = 2$.

Figure 5.- Variation of root-mean-square vertical-acceleration ratio with nondimensional time to damp to one-half amplitude.

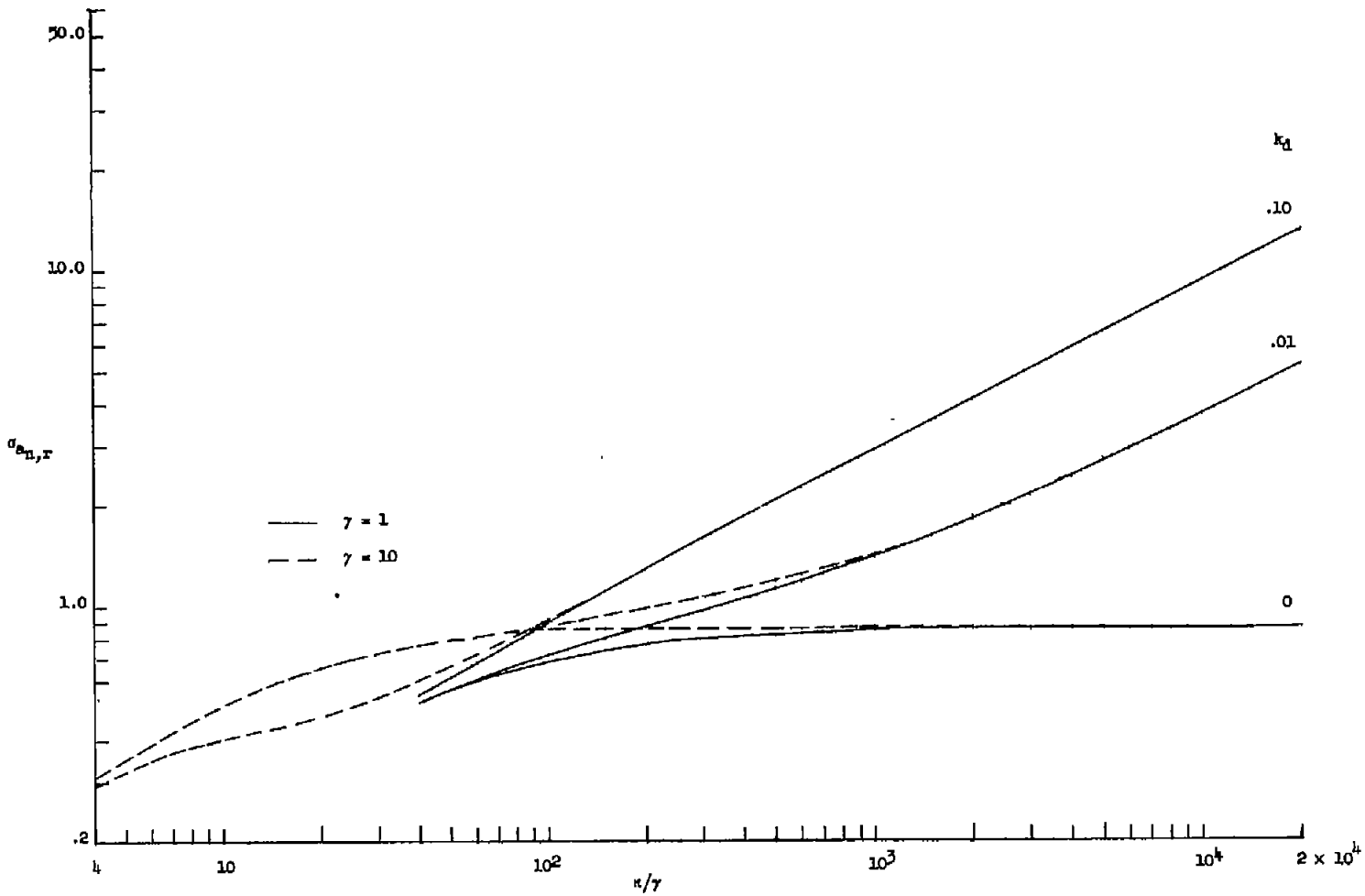

(b) $\kappa = 50$; $\gamma = 1$ and 10.

Figure 5.- Continued.

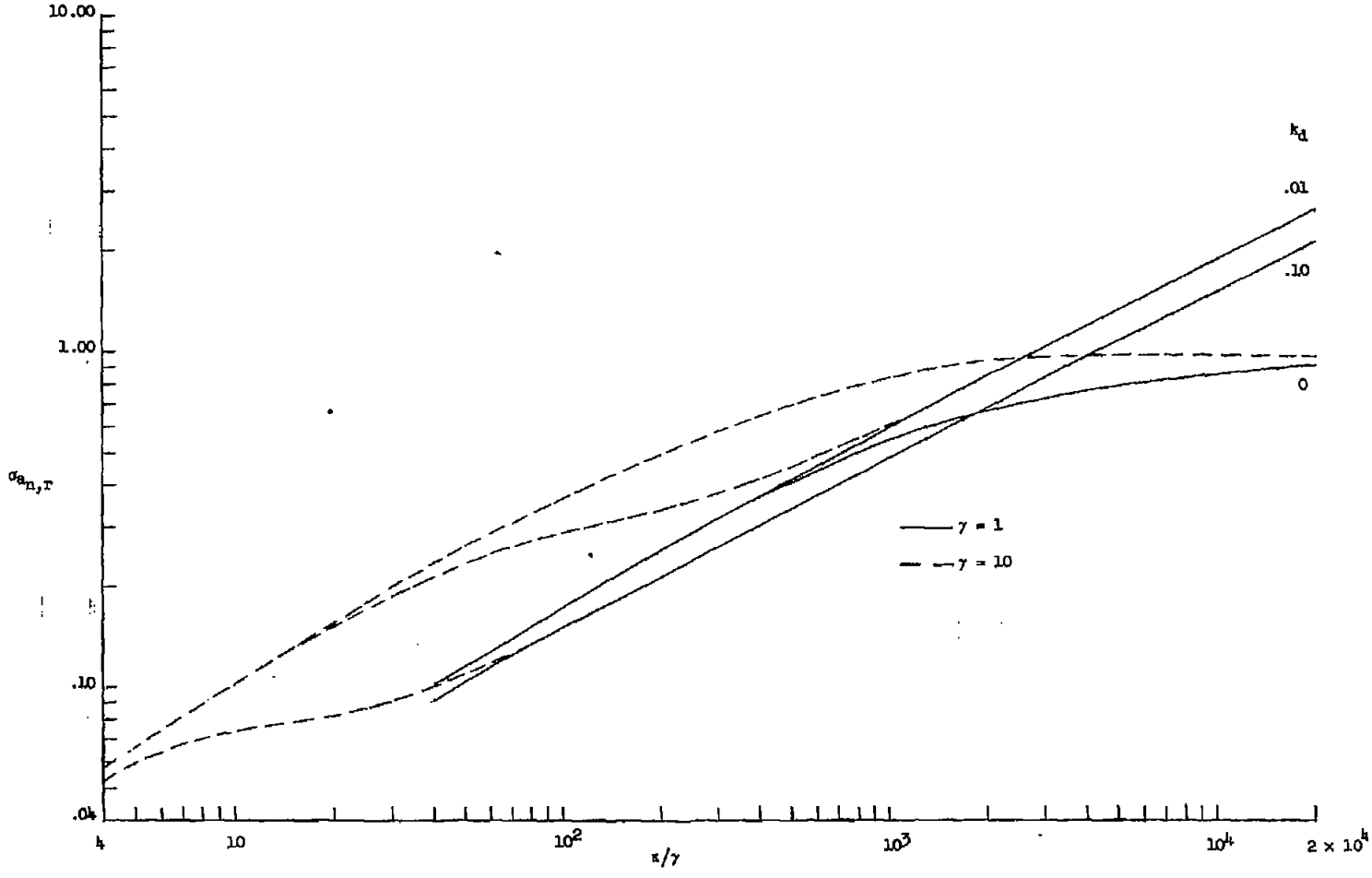

(c) $s = 2{,}000$; $\gamma = 1$ and 10.

Figure 5.- Concluded.

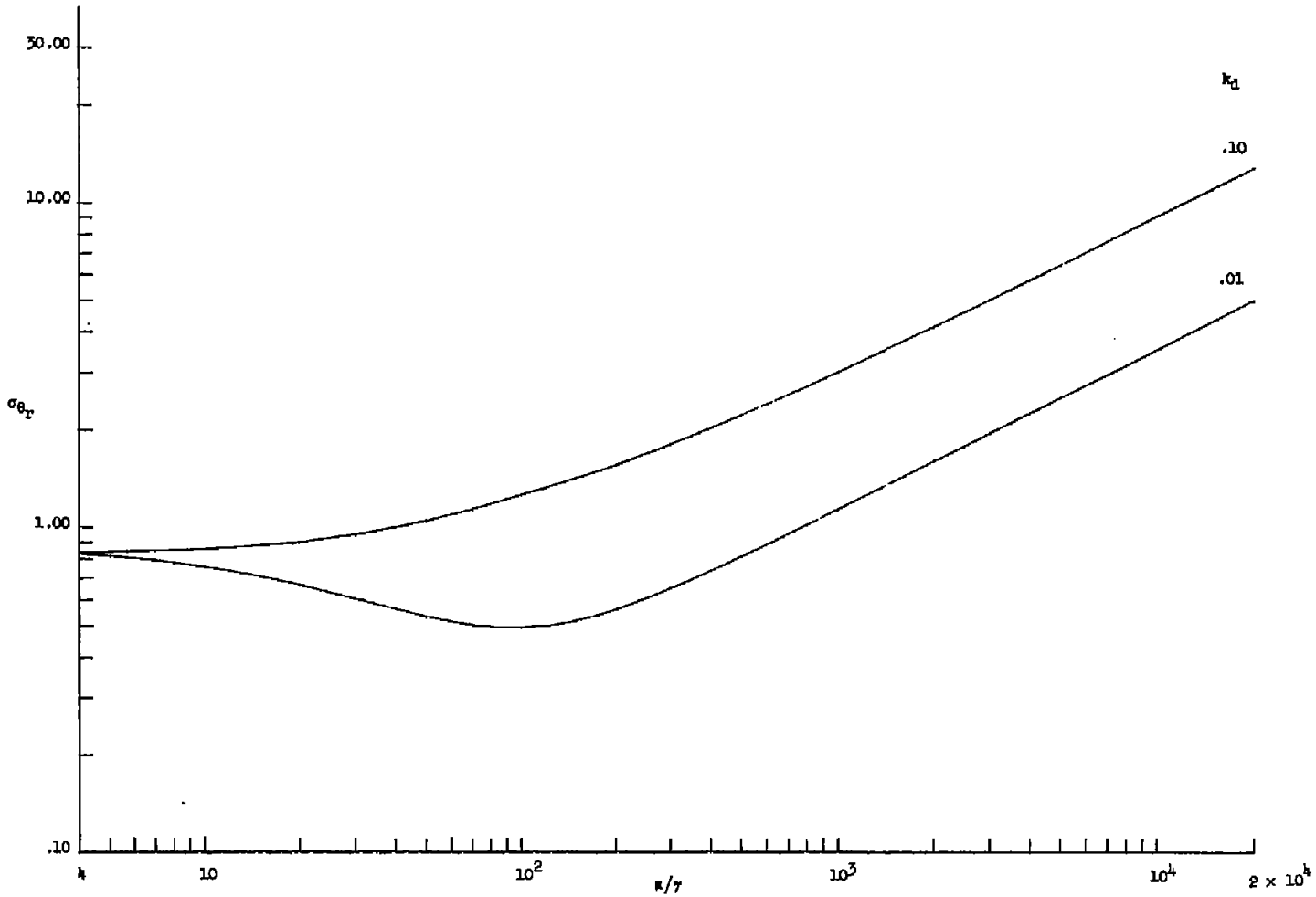

(a) s = 50.

Figure 6.- Variation of root-mean-square pitch-angle ratio with nondimensional time to damp to one-half amplitude.

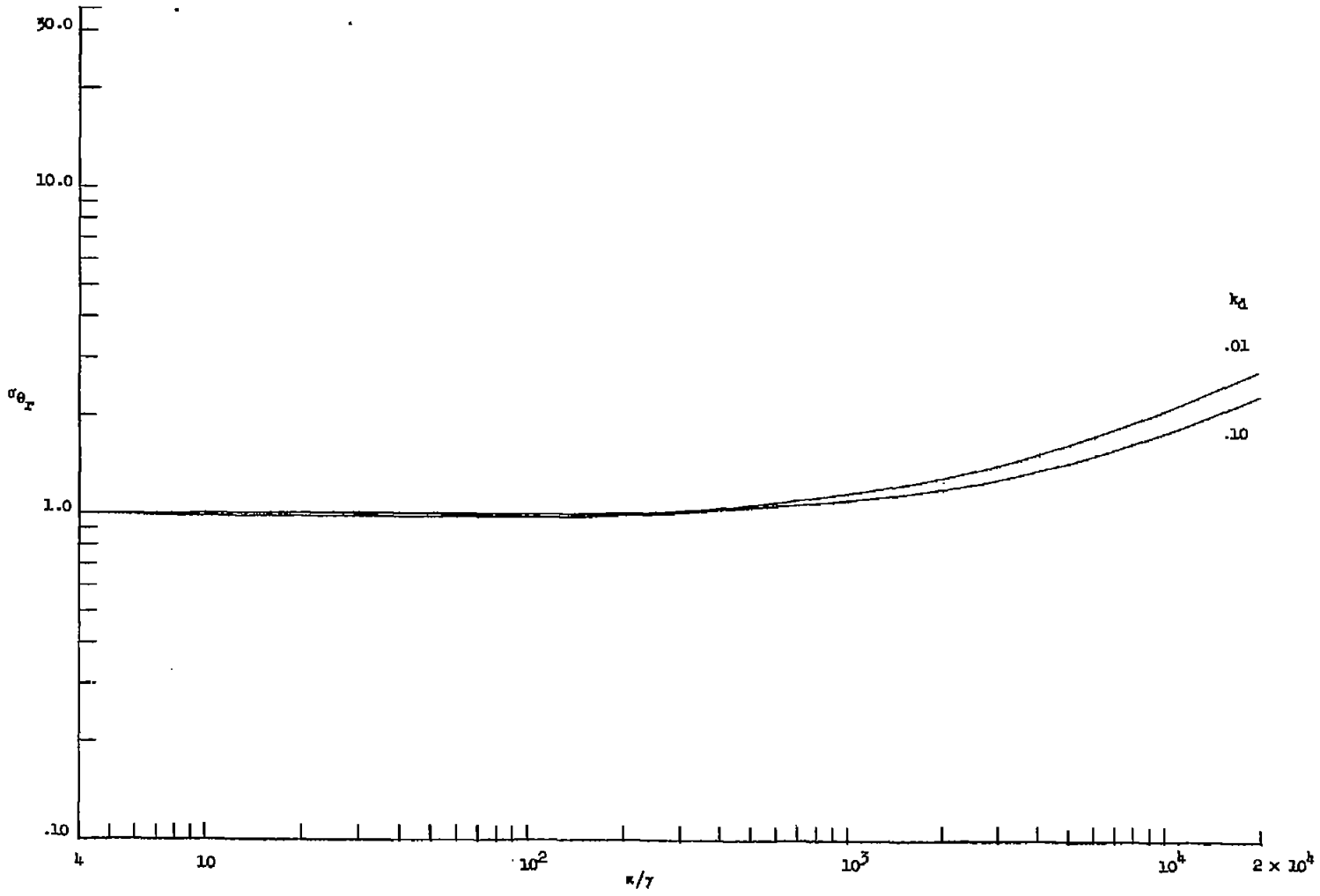

(b) s = 2,000.

Figure 6.- Concluded.

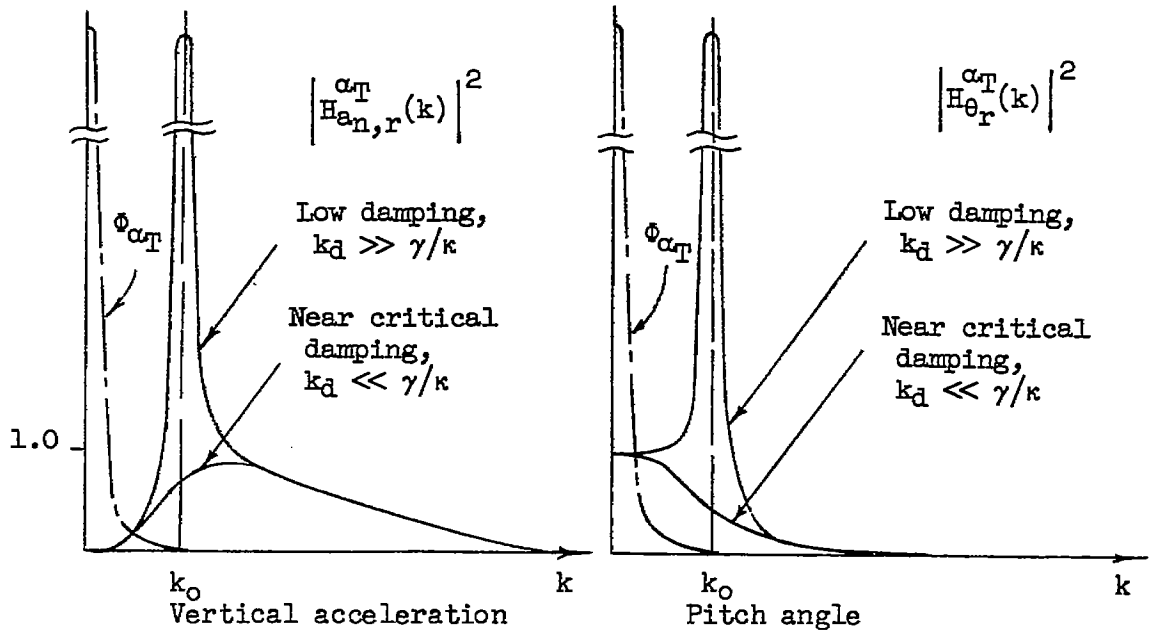

(a) Large relative-turbulence scale. $k_o s \gg 1.0$.

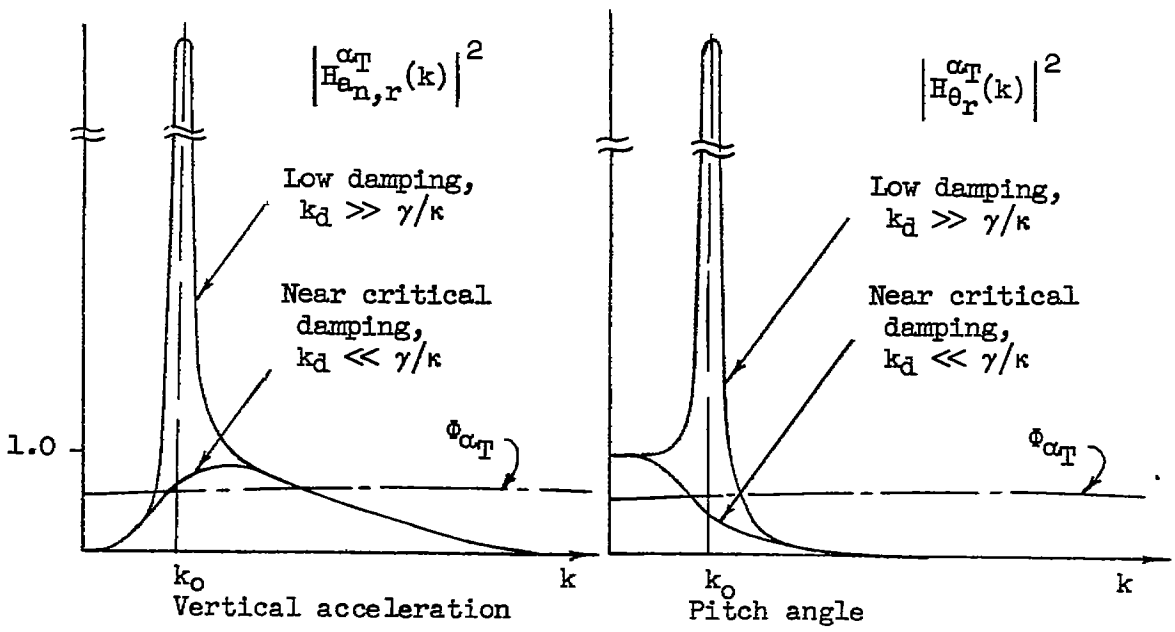

(b) Small relative-turbulence scale. $k_o s \ll 1.0$.

Figure 7.- Relationships between the transfer-function moduli and the power spectra for small and large relative-turbulence scales.